Chapter 2
Engineering Fundamentals of Balloons

Abstract Balloons are giant membrane structures that float in the thin atmosphere. This chapter first presents the geometric design problems for the balloon body. Specifically, the shape of axisymmetric natural-shape balloons is discussed, and this design concept is then extended to superpressure balloons that are reinforced by load tapes. Throughout this discussion, current progress in research on design concepts that dramatically enhance balloon strength is explained in detail. The dynamics of a balloon flight are governed by a complex combination of fluid dynamics and thermodynamics. A mathematical model that describes the motion of a balloon is derived. This model includes the effects of the aerodynamical forces acting on the balloon, and of the gas temperature variation caused by thermal conduction and radiation between the balloon and surrounding atmosphere, the sun, the ground, and outer space. The ascent, descent, and the lateral motion of balloons are then explained in detail.

2.1 Buoyant Force and Attainable Altitude of Balloons

2.1.1 Principle of Buoyancy

The fact that balloons float in the atmosphere is founded upon the principle of buoyancy discovered by Archimedes in the third century B.C. It states that "an object submerged in a fluid experiences an upward force that is equal to the weight of the same volume of fluid" [1]. This phenomenon can be explained as follows.

As shown in Fig. 2.1a, a rectangular solid is lowered into a fluid. According to Pascal's law, the object is subject to pressure from the fluid pressing on its surfaces in directions normal to its surfaces. The pressures on the sides are counterbalanced, so that the pressures acting on the upper and lower surfaces p_1 and p_2 are given by

$$p_1 = \rho g z_1, \tag{2.1}$$

N. Yajima et al., *Scientific Ballooning: Technology and Applications of Exploration Balloons Floating in the Stratosphere and the Atmospheres of Other Planets*,
DOI 10.1007/978-0-387-09727-5_2, © Springer Science+Business Media LLC 2009

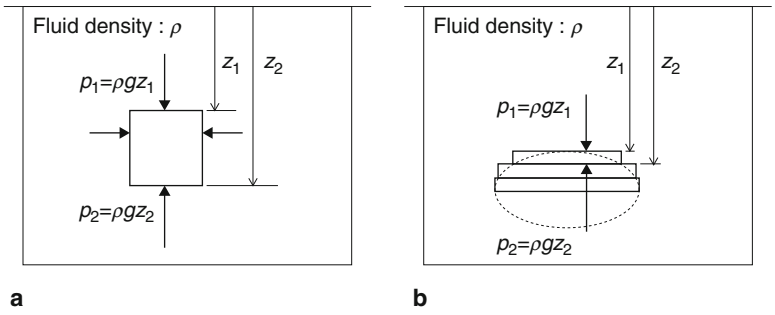

Fig. 2.1 Principle of buoyancy

$$p_2 = \rho g z_2, \tag{2.2}$$

where z_1 and z_2 are the respective depths of the upper and lower surfaces, ρ is the fluid density, and g is the acceleration due to gravity. Hence, if we take the area of the upper and lower surfaces to be S and the volume of the rectangular body to be V, the total sum of forces F in the upward direction that is imparted to the rectangular solid by the fluid is given by

$$F = p_2 S - p_1 S = \rho g(z_2 - z_1)S = \rho g V. \tag{2.3}$$

The same result can be obtained for an arbitrarily shaped body by summing thin horizontal slices (Fig. 2.1b) and applying (2.3) to each plate.

2.1.2 Effect of Buoyancy from a Gas

Consider the increase in the upward force if a buoyant gas of volume V is injected into a balloon. If we take ρ_a and ρ_g to be the densities of the external air and the internal buoyant gas, respectively, the increase in upward force acting on the balloon ΔF becomes

$$\Delta F = (\rho_a - \rho_g) g V. \tag{2.4}$$

The $\rho_a g V$ term on the right-hand side is the buoyant force from Archimedes' principle, and $\rho_g g V$ is the weight of the gas inside the balloon.

Thus, the contribution of the gas to the upward force is given by the difference between the density of the external air and that of the internal buoyant gas. For this reason, in subsequent descriptions, $\Delta\rho g V$ is referred to as the effective buoyant force and it is a function of the difference in the densities $\Delta\rho = \rho_a - \rho_g$.

2.1.3 Attainable Altitude

Balloons float to an altitude at which the buoyant force equals the total weight of the balloon system. Here the total weight of the balloon system includes the weight of the injected buoyant gas. The weight prior to charging with gas (i.e., the weight of the total system minus the weight of the buoyant gas) is referred to as the weight of the balloon system. If the definitions given in the above section are used, the balloon will float to an altitude at which the weight of the balloon system equals the effective lifting force.

Figure 2.2 shows the relationship between the attainable altitude and the mass of a balloon system for various balloon volumes. In this figure, the broken lines indicate different membrane thicknesses, and the solid lines represent different balloon volumes. The value on the horizontal axis at the intersection point of a solid and a broken line indicates the mass of the main balloon made from a membrane having the thickness indicated by the broken line. However, since the masses of balloons having the same volume may differ a little according to their precise specifications, the values given in this figure are simple approximations. For reference, open circles indicate the masses of some actual balloons.

If the balloon volume is specified, the mass of the balloon system can be determined from the desired attainable altitude. The total mass that can be carried is given by the difference between the total mass of the balloon system and the mass of the main balloon. In addition, the altitude given by the value on the vertical axis for the intersection point represents the maximum altitude that can be achieved if the balloon were to ascend with no payload attached. This demonstrates that it is important to lighten the mass of the main balloon in order to reach high altitudes.

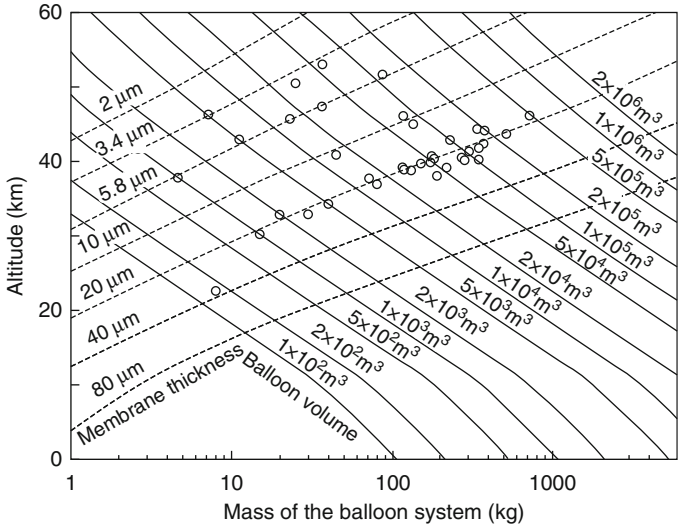

Fig. 2.2 Mass of the balloon system and attainable altitude

The polyethylene film used in scientific balloons is typically about 20 μm thick. For the case when a 100,000-m^3 balloon ascends to an altitude of 35 km, the total mass of the balloon system would be about 730 kg; subtracting the balloon mass (230 kg) from this value gives 500 kg as the total mass that can be carried. Although the balloon volume varies depending on payload weight and desired attainable altitude, the volumes generally used lie between a few thousand and a few hundred thousand cubic meters. The biggest operational balloon is a $1 \times 10^6\,m^3$ balloon used by NASA, which is able to carry an approximately 4-ton payload up to an altitude of 37 km. Another balloon is a $1.7 \times 10^6\,m^3$ balloon, which is able to carry a 700-kg payload up to an altitude of 49 km.

Polyethylene films with thicknesses of 6 μm or less are used in balloons designed to carry light payloads to high altitudes. These balloons carry payloads of 100 kg or less, and they are chiefly used for investigating special weather phenomena, for performing atmospheric and space observations, and for checking wind direction and wind speeds in advance in regions near or above 40 km when conducting high-altitude balloon experiments [2]. The ISAS attained a record altitude of 53 km using a 60,000 m^3 balloon made of a 3.4-μm-thick film and loaded with a light payload of about 5 kg [3].

Table Talk 1: How Archimedes Demonstrated the Existence of Buoyant Force

Balloon specialists should pay homage to the life of Archimedes, since ballooning is completely dependent on the principle of buoyancy, which he discovered.

So, how was it possible to demonstrate the existence of a buoyant force back in the third century B.C.? This is an interesting question. Fortunately, Archimedes' writings have been translated into many languages [1]. The fact that such ancient writings have been preserved is a miracle in itself and drives home their relevance to the scientific fields of Western civilization.

The proof of the buoyant force may be found in volume one of Archimedes' book entitled "On Floating Bodies," which contains two postulates and nine theses. The basis of this proof is that when the same substance as the fluid is placed in a fluid, it will neither sink nor float. That is, theses three and seven form the basis, which state that a substance becomes lighter by an amount equal to the weight of the substance immersed. Subsequently, a proof is given by citing examples and refining the principle. Of course, viewed from the perspective of modern science, it does not constitute a rigorous proof. However, one impressive point is the fact that a definition of a fluid is presented as the initial postulate (i.e., an assumed axiom). Since buoyancy is a phenomenon that occurs within fluids, Archimedes went through the very proper step of first defining a fluid. If the properties of a fluid had been pursued and extended to Pascal's theorem, then Archimedes' proof of buoyant forces would have been more complete. Next, it is necessary to demonstrate the basis for Pascal's definition (actually, this has been omitted in the present book as well).

Another surprise is found in thesis two, which states, "the fluid's surface assumes a form having the same center as the earth." It is thought it was already known in

the Greek period that the Earth was round. However, the fact that they knew that the surface of water is round suggests that they may have been one step away from discovering the concept of universal gravitation.

2.2 Balloon Configurations

2.2.1 Historical Background and Overview of Problems

With the exception of metal shell balloons that are designed to float in high-temperature and high-pressure environments such as Venus, balloon envelopes are generally made from flexible film (membranes), particularly the envelopes of stratospheric balloons. With the exception of rubber balloons, the increase in volume resulting from stretching of the film can be assumed to be negligible. Thus, the envelopes are manufactured from a lightweight, thin film in its fully expanded shape.

The shape design problem considers what the most appropriate balloon shape is. The following three points must be taken into account:

1. The transmission of the load of the suspended payload to the film should be distributed as uniformly as possible.
2. The balloon strength should be maximized in a way that minimizes the tensile force and that ensures that the tensile force is uniformly distributed on the film that is subject to pressure.
3. Maintaining the relationship of points (1) and (2) even when the shape of the balloon changes due to expansion during ascent.

In the 150 years from the first flight of balloons to the end of the 1930s, the shapes of balloons were not really studied theoretically and systematically in a way that took into account the three points stated above. The sphere was the most frequently used shape since it is best able to withstand pressure. Analyses in scientific books started with such an assumption (e.g., [4]). Other balloons having different shapes were also tried; these included balloons that were slightly deformed at the base of the sphere and long cylinders with hemispheres on the top and bottom.

The first step toward modern scientific ballooning was the concept of the natural-shape balloon proposed by R.H. Upson, which is presented in detail in Sect. 2.2.2. Other shapes are briefly described to demonstrate the superiority of his proposed shape over other shapes.

2.2.1.1 Spherical Balloons

If the weight and buoyant force of the membrane are neglected, the spherical shape gives rise to a uniform biaxial tension in the membrane over the entire surface of the pressurized balloon. For a tension T, a pressure on the membrane P, and a radius r, we have

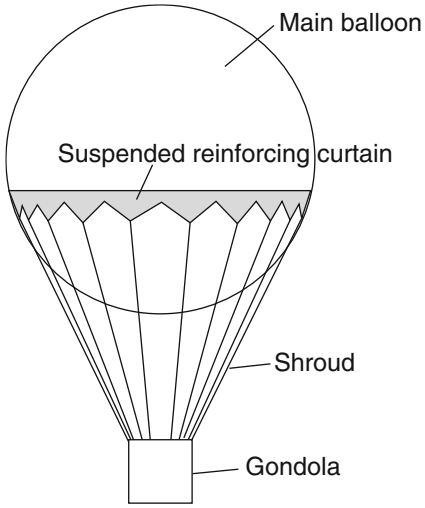

Fig. 2.3 Classical method for suspending a payload. Multiple ropes (called a shroud) are hung from the cloth that is installed like a curtain a little below the balloon's equator, and the payload is suspended at the lowest point. The balloon of Piccard mentioned in Sect. 2.1.1 followed this design

$$T = \frac{rP}{2}. \tag{2.5}$$

At first glance, it might appear that a spherical balloon minimizes the load on the membrane and is the optimal shape for a pressurized balloon. It also has the smallest surface area for a given volume, thus complying with the demand to minimize the weight.

However, there are several problems associated with spherical balloons. The first problem is that there is no single point for suspending a heavy load, since the entire surface of the balloon consists of a thin, uniform membrane. Consequently, the bottom of the balloon has to be locally reinforced, or a net needs to be draped over the upper half of the balloon as shown in the illustrations of classic balloons shown in Figs. 1.2 and 2.3. Alternatively, a curtain is attached around the equatorial line, and multiple ropes (called a shroud) are hung from this area; a payload is then suspended from the ends of the ropes, which has the effect of distributing the load.

The second problem is that on the ground and during ascent the balloon is only partially expanded, and thus its shape differs from a perfect sphere. During these times, the tension in the membrane will be nonuniformly distributed. For these reasons, spherical balloons are useful only for small balloons with light payloads.

2.2.1.2 Cylindrical Balloons

A cylindrical balloon is the one in which the central section of the envelope forms a long cylinder and the upper and lower ends are closed off in some form. They are useful for cases when it is easy to form a cylinder out of the membrane (or when the

membrane is initially formed into a thick tube). The circumferential tensile forces that act on the cylindrical section in the circumferential direction are given by the product of the pressure differential on the membrane and the radius of the cylinder. The sum total of the tensions acting parallel to the cylinder's axis is given by the product of the pressure and the cross-sectional area of the cylinder.

The longer and narrower the shape is, the greater the pressure resistance becomes; however, the volume to surface area ratio becomes worse. In a large stratospheric balloon, in contrast to a spherical balloon, the weight of the balloon itself is large and this is a disadvantage. However, this shape is suitable when there is a large lifting force per unit volume, such as in the high-density, low-altitude atmosphere of Venus.

2.2.1.3 Tetrahedral Balloon

A balloon constructed in the shape of a regular tetrahedron is called a tetrahedral balloon (Fig. 2.4). Because it lacks rotational symmetry, at first it appears to be an unnatural shape for a balloon. But since it has features such as a flat top and a bottom that converges to an acute angle, in some major points it resembles natural-shape balloons that are discussed later. Its shape consists of a cylinder with a length that is equal to half the circumference multiplied by cos 30°, and both ends may be closed off in directions orthogonal to each other.

As a result, since small balloons are easy to manufacture, they are used as auxiliary balloons at CNES for suspending a gondola on the ground (Fig. 2.4). Refer to Sect. 3.4.2 for details on the launch method.

2.2.1.4 Natural-Shape Balloons

Spherical balloons, cylindrical balloons, and tetrahedral balloons all assume their designed geometries only when they become fully inflated after ascent. When they are injected with gas on the ground, only a portion of their top section is inflated. R.H. Upson noticed that in the partially inflated section, there are a large number of folds parallel to the longitudinal axis, as can be seen in Fig. 2.5. This is because there is excess film in the circumferential direction. That is, because the length of the film in the longitudinal direction is constant irrespective of the state of expansion, no tension is generated in the film in the circumferential direction. Upson formulated a balloon shape by assuming only a longitudinal tension. He published a seminal paper on this concept in 1939 [5]. Upson obtained the idea for a natural-shape balloon by observing that a large number of folds are formed parallel to the longitudinal axis due to the excess film in the balloon.

If only an infinitesimal amount of excess film remains in the circumferential direction at full inflation, a balloon shape can be formulated that maintains the same type of shape from partial inflation through to full inflation. Subsequently, this proposed shape (which came to be known as the natural-shape balloon) played a major role in advancing ballooning from an era of trial and error to an era of scientific research.

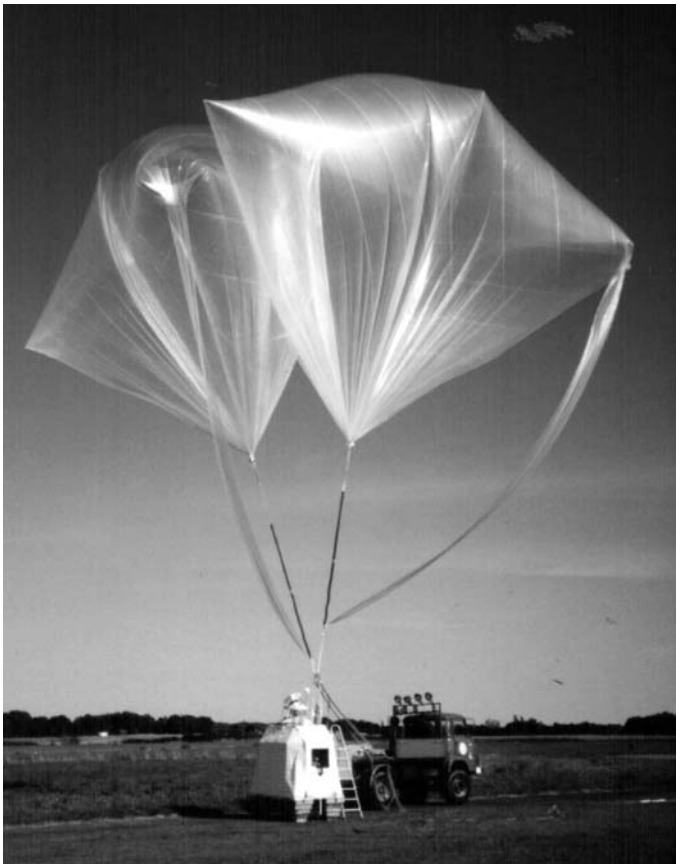

Fig. 2.4 Tetrahedral balloons being used by CNES. (in this example, two tetrahedral balloons are being used.) (courtesy of CNES)

However, although the formula expressing the shape has a simple form (see later discussion), it cannot be solved analytically. Upson was only able to achieve a similar form through using an approximation. Attempts were made in the 1940s to determine a solution by using an analog computer to draw the balloon shape with a pen recorder; this work was done at the University of Minnesota, which was one of the driving forces behind balloon development in US. In the early 1960s, Smalley at the NCAR systematically derived accurate balloon shapes for various conditions by performing numerical calculations using a digital computer, which had reached a usable stage. These solutions were applied extensively to designing actual balloons [6].

The natural balloon shape, which was first formulated by Upson and then practically realized by Smalley, is a completely rotationally symmetrical body made only of film. At around the same time, fiber reinforcement technology, which involves vertically inserting bundles of high-strength reinforcing fibers (called load tapes) at fixed intervals, started to be applied in the construction of large balloons (Fig. 1.4).

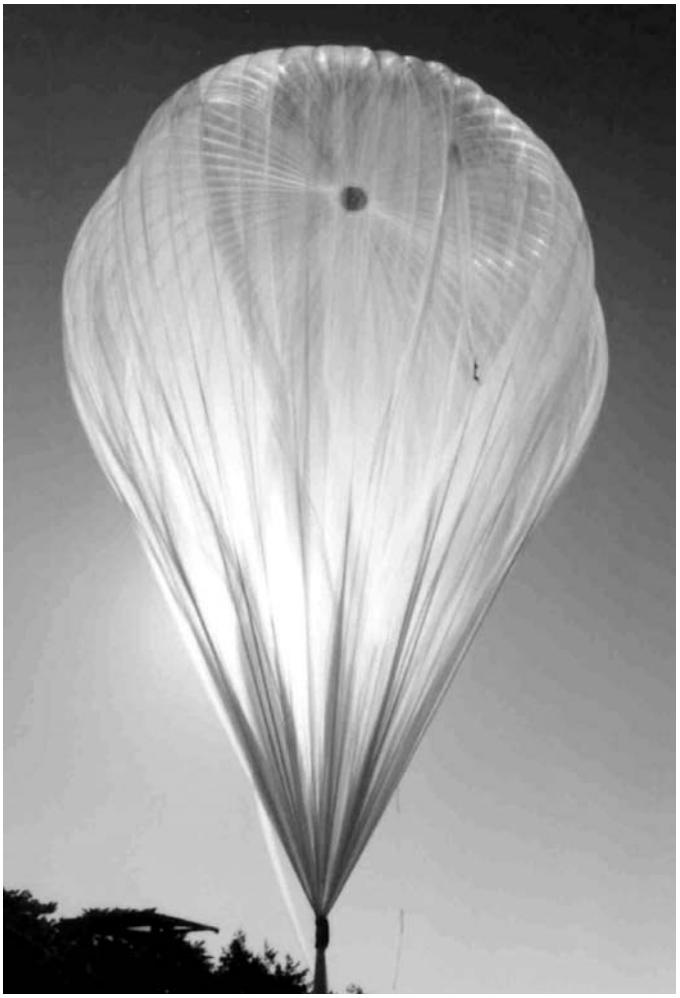

Fig. 2.5 Top of a balloon partially inflated on the ground

This technology increases the envelope's resistance to pressure, enabling heavier payloads to be suspended. In this case, because localized distortions in the film form between adjacent load tapes, the lateral cross section of the envelope is not a perfect circle (Fig. 2.19) and the balloon shape is no longer rotationally symmetrical. Naturally, the film tension is not uniaxial in the meridional (i.e., longitudinal) direction, but it is biaxial in the both the circumferential and meridional directions. However, the overall balloon shape can be viewed as being approximately the natural shape. As a result, problems arising from differences between actual balloons with and without load tapes were disregarded, and were not fully elucidated.

In 1998, two of the authors of this book (N. Yajima and N. Izutsu) reexamined the shape design problem starting from its fundamentals, and they proposed the

"three-dimensional (3D) gore design concept" [7]. This concept involves intentionally forming bulges having small local radii between adjacent load tapes. In this concept, the distinction between the roles of the load tape and the film are well defined, namely the load tape receives all of the forces in the meridional direction, and the film receives the forces generated by the pressure as an uniaxial tension in the circumferential direction. Since only a uniaxial tension is generated in the film, this concept both inherits and advances Upson's concept, and enables a consistent understanding of the balloon-shape design problem, both for cases when a load tape is present and when it is absent.

Moreover, this concept can be used to optimize the tension generated in the film to a small constant amount that is independent of the balloon volume. A super-pressure balloon, which requires a high resistance to pressure, becomes feasible by applying this extended natural balloon shape design concept, since a balloon can be made by rational design making use of a thin, lightweight film if necessary. The 3D gore design concept solves a longstanding issue of how to construct a practical super-pressure balloon. In the following section, we give a detailed mathematical description of the natural-shape balloon concept, which represents the foundation of balloon shape design.

2.2.2 Natural-Shape Balloon Concept

As the shape a in Fig. 2.6 shows, at the time of launch a balloon is partially inflated with the lifting gas only in one section. As it ascends into the sky, it expands in the manner shown by the shape b, and ultimately becomes the fully inflated shape c in the figure when it attains its level flight altitude.

In this section, we determined the shape of balloons made of film, the stretching of which is small enough to be ignored, and the process by which these balloons expand in the manner described above. In the first stage in this section, no load tape is inserted for reinforcement, and an axisymmetric (i.e., rotationally symmetrical) shape is considered. A description extending to balloons that do have load tape is presented in Sect. 2.2.3.

2.2.2.1 General Expression where there is Biaxial Tension

Generally, only biaxial tensile stresses are considered to act on thin films such as those in balloons, and other stresses (i.e., compressive and shear stresses) can be disregarded. Thus, we first formulate the shape for the case when biaxial forces act in the film as a generalization for determining the natural-shape balloon described in the previous section.

As shown in Fig. 2.7, the balloon film can be represented by the curved surface formed when curve C is rotated around the A-axis. The origin for curve C having an axis of rotation A is set to be the base or nadir of the balloon P_1, and its endpoint

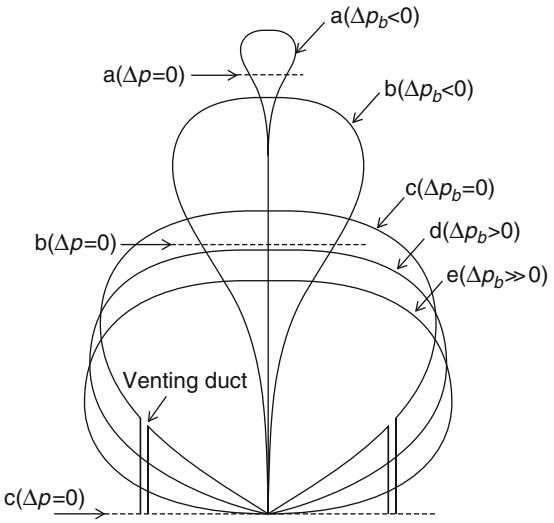

Fig. 2.6 The typical shapes of balloons categorized as a natural-shape balloon. Shape a and b show partial inflation; shape c shows full inflation of a zero-pressure balloon; shape d and e show instances when the balloon internal pressure is greater than the surrounding atmospheric pressure (super-pressure balloon). The *dotted lines* at $\Delta p = 0$ indicate the heights at which the pressures inside and outside the balloon are the same

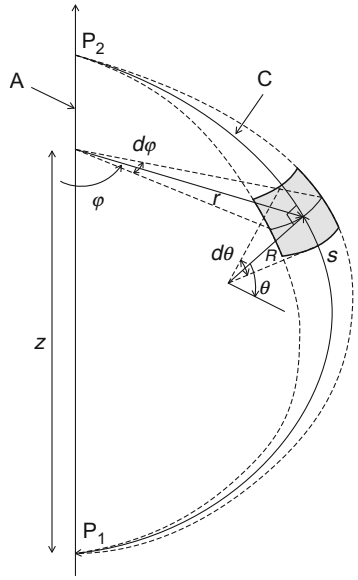

Fig. 2.7 Definition of the surface element on the balloon envelope that is formed by rotating curve C around axis A

is the apex of the balloon P_2. The length from P_1 along the curve C is represented by s. The overall length of curve C is designated as the length of the balloon and is represented by ℓ_s. The radius of curvature of curve C is denoted by R, the angle formed by the line tangent to curve C and the axis of rotation is denoted by θ, and the distance from curve C to the axis of symmetry A is denoted by r. In addition, as shown in the figure, the height from P_1 at the base of the balloon to each point on curve C is represented by z. The height of point P_2 (i.e., the distance $P_1 - P_2$) is referred to as the height of the balloon. In addition, the maximum value of r is represented by $r_{\max}$, and the value for $2r_{\max}$ is called the balloon diameter.

The angle in a plane perpendicular to the rotational axis A is φ, and the dynamic balance for surface element $r\mathrm{d}\varphi R\mathrm{d}\theta(= r\mathrm{d}\varphi\mathrm{d}s)$ depicted in Fig. 2.7 is considered. The tension per unit length acting on this section of element (Fig. 2.8) is represented by T_θ over surfaces of constant φ and by T_φ over surfaces of constant θ. The actual mass per unit area of balloon film is taken to be w_e, and the difference between the internal pressure of the balloon and the surrounding atmospheric pressure is Δp (Δp is defined to be positive when the internal pressure is higher than atmospheric pressure). Thus, balancing equations for the z direction and the r direction gives (2.6) and (2.7), respectively.

$$\begin{aligned}&(T_\theta + \frac{\mathrm{d}T_\theta}{2})(r+\frac{\mathrm{d}r}{2})\mathrm{d}\varphi\cos(\theta+\frac{\mathrm{d}\theta}{2}) - (T_\theta - \frac{\mathrm{d}T_\theta}{2})(r-\frac{\mathrm{d}r}{2})\mathrm{d}\varphi\cos(\theta-\frac{\mathrm{d}\theta}{2}) \\ &\quad -r\mathrm{d}\varphi w_e g\mathrm{d}s - r\mathrm{d}\varphi\Delta p\mathrm{d}s\sin\theta = 0\end{aligned}, \quad (2.6)$$

$$\begin{aligned}&(T_\theta + \frac{\mathrm{d}T_\theta}{2})(r+\frac{\mathrm{d}r}{2})\mathrm{d}\varphi\sin(\theta+\frac{\mathrm{d}\theta}{2}) - (T_\theta - \frac{\mathrm{d}T_\theta}{2})(r-\frac{\mathrm{d}r}{2})\mathrm{d}\varphi\sin(\theta-\frac{\mathrm{d}\theta}{2}) \\ &\quad -2T_\varphi\mathrm{d}s\sin\frac{\mathrm{d}\varphi}{2} + r\mathrm{d}\varphi\Delta p\mathrm{d}s\cos\theta = 0\end{aligned}, \quad (2.7)$$

where g is the acceleration due to gravity.

Rearranging (2.6) and (2.7) by eliminating the higher-order terms yields the following.

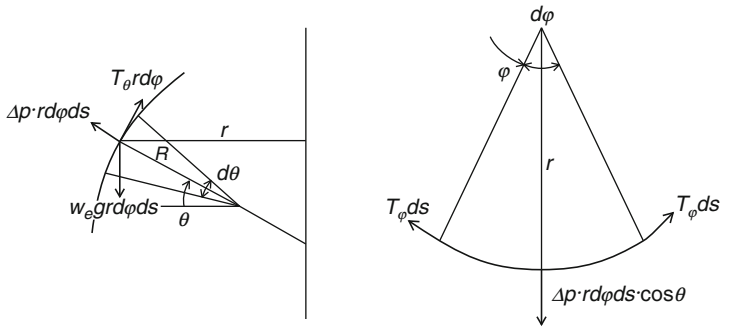

a Cross-section including the axis of rotation

b Cross-section perpendicular to the axis of rotation

Fig. 2.8 Tension and pressure acting on a surface element of the balloon: **a** Cross-section including the axis of rotation; **b** Cross-section perpendicular to the axis of rotation

$$\frac{\mathrm{d}(rT_\theta)}{\mathrm{d}s}\cos\theta - rT_\theta \sin\theta \frac{\mathrm{d}\theta}{\mathrm{d}s} - rw_e g - \Delta pr\sin\theta = 0, \tag{2.8}$$

$$\frac{\mathrm{d}(rT_\theta)}{\mathrm{d}s}\sin\theta + rT_\theta \cos\theta \frac{\mathrm{d}\theta}{\mathrm{d}s} - T_\varphi + \Delta pr\cos\theta = 0. \tag{2.9}$$

Further rewriting (2.8) and (2.9) gives the following.

$$rT_\theta \frac{\mathrm{d}\theta}{\mathrm{d}s} = T_\varphi \cos\theta - rw_e g\sin\theta - \Delta pr, \tag{2.10}$$

$$\frac{\mathrm{d}(rT_\theta)}{\mathrm{d}s} = T_\varphi \sin\theta + rw_e g\cos\theta. \tag{2.11}$$

At the same time, if the density of the atmosphere and the density of gas inside the balloon are denoted by ρ_a and ρ_g respectively, Δp can be expressed as

$$\Delta p = \Delta p_\mathrm{b} + (\rho_a - \rho_g)gz. \tag{2.12}$$

Here, Δp_b is the pressure difference at the base of the balloon $\mathrm{P}_1(s = r = z = 0)$.

If the height at the point where $\Delta p = 0$ is set to z_b, (2.12) becomes

$$\Delta p = (\rho_a - \rho_g)g(z - z_b) \tag{2.13}$$

and (2.10) becomes

$$rT_\theta \frac{\mathrm{d}\theta}{\mathrm{d}s} = T_\varphi \cos\theta - rw_e g\sin\theta - b_g(z - z_b)r, \tag{2.14}$$

where b_g represents the effective buoyant force per unit volume (the net upward force) produced by the difference in the densities of the surrounding atmosphere and the lifting gas. That is

$$b_g = (\rho_a - \rho_g)g. \tag{2.15}$$

In addition,

$$\frac{\mathrm{d}r}{\mathrm{d}s} = -\sin\theta, \tag{2.16}$$

$$\frac{\mathrm{d}z}{\mathrm{d}s} = \cos\theta \tag{2.17}$$

are found from geometrical considerations. At the same time, the geometric surface area S and volume V for the object formed from the curved surface generated by rotating curve C around the A axis may be determined by

$$\frac{\mathrm{d}S}{\mathrm{d}s} = 2\pi r, \tag{2.18}$$

$$\frac{\mathrm{d}V}{\mathrm{d}s} = \pi r^2 \cos\theta. \tag{2.19}$$

2.2.2.2 Formula Describing the Natural-Shape Balloon

In Upson's concept as described in Sect. 2.2.1.4, there is excess film in the φ-direction in the shape of the balloon in the process of becoming fully inflated. In this condition, folds or wrinkles form parallel to the meridian, and there is no tension in the φ-direction of the film across these folds or wrinkles. Consequently, by setting $T_\varphi = 0$ in (2.14) and (2.11), the following two equations that describe the vertical cross-section of a natural-shape balloon can be obtained.

$$rT_\theta \frac{\mathrm{d}\theta}{\mathrm{d}s} = -rw_e g \sin\theta - b_g(z - z_b)r, \tag{2.20}$$

$$\frac{\mathrm{d}(rT_\theta)}{\mathrm{d}s} = rw_e g \cos\theta. \tag{2.21}$$

If it is assumed that there is an infinitesimal excess in the film in the φ-direction even when the balloon is fully inflated, these equations can be used for all stages, from the gas being injected into the balloon at launch through to full inflation.

We set $-F_1$ to be the force in the z-direction acting at the base of the balloon P_1 (downward force from the payload suspended from the bottom of the balloon), and we set $-F_2$ to be the force in the z-direction acting in the same way at the apex of the balloon P_2 (generally, $F_1, F_2 \geq 0$).

Here, the dimensionless length λ is defined as

$$\lambda = \left(\frac{F_1 + F_2}{b_g}\right)^{\frac{1}{3}}, \tag{2.22}$$

and the following dimensionless parameters are defined.

$$\tilde{r} = \frac{r}{\lambda},\ \tilde{z} = \frac{z}{\lambda},\ \tilde{z}_b = \frac{z_b}{\lambda},\ \tilde{s} = \frac{s}{\lambda},\ \tilde{\ell}_s = \frac{\ell_s}{\lambda},\ \tilde{R} = \frac{R}{\lambda}, \tag{2.23}$$

$$\tilde{T}_\theta = \frac{T_\theta}{b_g \lambda^2}, \tag{2.24}$$

$$\tilde{S} = \frac{S}{\lambda^2}, \quad \tilde{V} = \frac{V}{\lambda^3}. \tag{2.25}$$

Equations (2.20) and (2.21) may be written as follows.

$$\tilde{r}\tilde{T}_\theta \frac{\mathrm{d}\theta}{\mathrm{d}\tilde{s}} = -k\Sigma_e \tilde{r}\frac{\mathrm{d}\tilde{r}}{\mathrm{d}\tilde{s}} - (\tilde{z} - \tilde{z}_b)\tilde{r}, \tag{2.26}$$

$$\frac{\mathrm{d}(\tilde{r}\tilde{T}_\theta)}{\mathrm{d}\tilde{s}} = k\Sigma_e \tilde{r}\frac{\mathrm{d}\tilde{z}}{\mathrm{d}\tilde{s}}, \tag{2.27}$$

where

$$k = (2\pi)^{-\frac{1}{3}}, \tag{2.28}$$

where Σ_e is the dimensionless film weight, and it is an important similarity parameter defined by

$$\Sigma_e = \frac{w_e g}{k b_g \lambda} \tag{2.29}$$

that characterizes the shape of the balloon. That is, because Σ_e is the only shape parameter in (2.26) and (2.27), shapes having the same value of Σ_e will result in similarly shaped balloons. In addition, (2.16) to (2.19) can be written as follows.

$$\frac{d\tilde{r}}{ds} = -\sin\theta, \quad \frac{d\tilde{z}}{d\tilde{s}} = \cos\theta, \tag{2.30}$$

$$\frac{d\tilde{S}}{d\tilde{s}} = 2\pi\tilde{r}, \quad \frac{d\tilde{V}}{d\tilde{s}} = \pi\tilde{r}^2\frac{d\tilde{z}}{d\tilde{s}}. \tag{2.31}$$

2.2.2.3 Significance of the Natural-Shape Balloon

As will be described in the next section, the radius of curvature becomes infinite and the surface becomes flat at the apex of the balloon. Consequently, in the partially inflated state during ascent, there is no part of the film where there is a shortage of length in the circumferential direction. Consequently, the balloon maintains a reasonable shape from ascent until full inflation.

As noted above, the reason why it is possible to calculate the shape with the circumferential tensile force $T_\varphi = 0$ as a constraint condition is because of the unique properties of the film material (i.e., the membrane). That is, in general an extremely thin and flexible membrane has no resistance to bending and no compressive forces in axially symmetric balloon shapes, as specified as a formulation assumption. If the length along the meridian line of the balloon envelope is constant and if it is assumed that there is some film slightly in excess of the required amount in the circumferential direction, there will be wrinkles generated parallel to the meridian line, and there will be no circumferential film tension perpendicular to these wrinkles. This is an important precondition for realizing natural-shape balloons.

This model is theoretically realized by neglecting stretching of the film; it is a statically determinate problem in structural mechanics, and it has the characteristic that it can be treated by considering shape and film extension separately.

2.2.2.4 Natural-Shape Balloons having Zero or Negative-Pressure Differential at the Base

The Case of Zero-Pressure Differential at the Base

The example below shows the case when $F_2 = 0$. First, treating the total length of the balloon $\tilde{\ell}_s$ as a constant, shapes with a pressure differential of 0 at the base of the

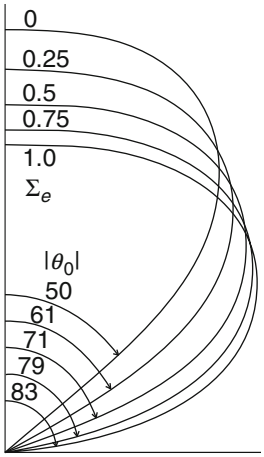

Fig. 2.9 Changes in the cross-sectional shape of a natural-shape balloon. The changes in the angle θ_0 at the base of the balloon are shown as a function of the similarity parameter Σ_e

balloon ($\tilde{z}_b = 0$) as determined by changing the similarity parameter Σ_e are shown in Fig. 2.9. This is obtained by determining θ_0 by repeated computation from the initial conditions

$$\tilde{r} = \tilde{z} = \tilde{S} = \tilde{V} = 0, \quad \tilde{r}\tilde{T}_\theta = \frac{1}{2\pi \cos\theta_0} \qquad (\tilde{s} = 0), \tag{2.32}$$

which when integrated becomes

$$\tilde{r} = 0 \qquad (\tilde{s} = \tilde{\ell}_s) \tag{2.33}$$

by assuming a θ_0 value for the angle θ at the computational starting point $\tilde{s} = 0$ based on the given parameter Σ_e.

At the apex of the balloon (i.e., at $\tilde{s} = \tilde{\ell}_s$) the radius of curvature is infinite, and the balloon is flat. The condition $\tilde{z}_b = 0$ (i.e., at the base of the balloon P_1 the pressure differential, $\Delta p_b = 0$) can be easily satisfied by setting the bottoms of venting ducts (which are installed in the lower part of the balloon (see shape c in Fig. 2.6) and are open at the bottom to the atmosphere) at the same height as the base of the balloon. This form of balloon is categorized as a zero-pressure balloon and it will be described in detail in Sect. 2.3.1.

Here, smaller Σ_e values indicate the fully inflated condition of a balloon that has a heavy payload compared with the film weight. The major difference in shape caused by differences in Σ_e is the angle at the base of the balloon. This relationship is depicted in Fig. 2.9. This relationship implies that shape varies with payload mass even for balloons having the same volumes and made from the same film.

The Case of Negative-Pressure Differential at the Base (Partial Inflation)

Next, we determine the shape during ascent. By taking the value of Δp_b to be negative (i.e., letting $\tilde{z}_\mathrm{b}$ be positive) this case can be determined in a similar way to those cases previously shown by the shape a and b in Fig. 2.6. Since there are the two parameters θ_0 and $\tilde{z}_\mathrm{b}$ in this calculation, the two convergence conditions in the iterative calculation are given in (2.33) and the fact that the volume $\tilde{V}$ is a prescribed value determined from the total mass and altitude of the balloon.

Since there is excess balloon film in this case, it is necessary to note that w_e is not a constant value, rather it depends on the distance from the base s. More specifically, we first determine the circumferential length ℓ_φ for each section of the balloon in its fully inflated shape.

$$\ell_\varphi(s) = 2\pi r. \tag{2.34}$$

Then w_e is also a function of s, and

$$\frac{\ell_\varphi}{2\pi r} w_e \tag{2.35}$$

may be substituted for w_e in (2.20) and (2.21).

2.2.2.5 Natural-Shape Balloons with a Positive Pressure Differential at the Base

When There is a Finite Pressure Differential at the Base

Next, we consider enclosed balloons without venting ducts where the pressure at the base of the balloon is greater than the surrounding atmospheric pressure. In other words, we consider the case when $\Delta p_\mathrm{b} > 0 \quad (z_\mathrm{b} < 0)$. The shape is determined by the procedure described in Sect. 2.2.2.4, and as Δp_b increases from 0, the balloon becomes oblate in shape, and is referred to as a pumpkin balloon (see the shape d in Fig. 2.6).

When the Pressure Differential at the Base is Infinite

At sufficiently high pressure differentials (i.e., when balloon internal pressure can be regarded as being independent of height) the force due to the weight of the film may be ignored, and the balloon reaches the limit shape shown by the shape e in Fig. 2.6. This shape is obtained by replacing $\tilde{z} + \tilde{z}_\mathrm{b}$ by the constant value $\tilde{z}_\mathrm{b}$ in (2.26) and (2.27) and setting $\Sigma_\mathrm{e} = 0$, and it is described by the following two equations.

$$\tilde{T}_\theta \frac{\mathrm{d}\theta}{\mathrm{d}\tilde{s}} = \tilde{z}_\mathrm{b}, \tag{2.36}$$

$$\frac{\mathrm{d}(\tilde{r}\tilde{T}_\theta)}{\mathrm{d}\tilde{s}} = 0. \tag{2.37}$$

The shape determined analytically from these equations is also the shape that has the maximum volume based on the constraint that the length of the meridian line is constant.

Here, (2.37) implies that the total value of $\tilde{T}_\theta$ in the cross section of fixed height $\tilde{z}$ is constant, being independent of $\tilde{z}$. Consequently, if we consider the equatorial region where $\tilde{r}$ is a maximum ($\tilde{r} = \tilde{r}_{\max}$), because it is symmetrical about the equator, the total value of tension for this section may simply be considered to be balanced with the force acting on this cross section due to the pressure differential inside and outside the balloon (here a constant value). In short,

$$2\pi\tilde{r}\tilde{T}_\theta = \pi\tilde{r}_{\max}^2(-\tilde{z}_b), \tag{2.38}$$

or expressed another way

$$\tilde{r}\tilde{T}_\theta = -\frac{\tilde{z}_b}{2}\tilde{r}_{\max}^2. \tag{2.39}$$

Accordingly, substituting (2.39) into (2.36) gives

$$\frac{\mathrm{d}\theta}{\mathrm{d}\tilde{s}} = -\frac{2\tilde{r}}{\tilde{r}_{\max}^2}. \tag{2.40}$$

This equation is called Euler's elastica [8]. This shape can be used to approximate the shape of super-pressure balloons. The radius of curvature along the meridian in the equatorial section of this balloon is half the radius $\tilde{r}_{\max}$ in the horizontal direction in the same section of the balloon.

$$\tilde{R} = \frac{\mathrm{d}\tilde{s}}{\mathrm{d}\theta} = \frac{\tilde{r}_{\max}}{2} \qquad (\tilde{r} = \tilde{r}_{\max}). \tag{2.41}$$

2.2.2.6 Film Tensile Force and Singularity

The film tension $\tilde{T}_\theta$ determined as above and the change with film position $\tilde{s}/\tilde{\ell}_s$ of the total value $2\pi\tilde{r}\tilde{T}_\theta$ are shown in Fig. 2.10. This corresponds with the shapes during inflation shown by the shape a to c in Fig. 2.6. The situation is depicted in which the tension $\tilde{T}_\theta$ abruptly increases near the top and bottom of the balloon. In addition, one can see that the tension increases as the balloon approaches full inflation.

Figure 2.11 shows the change in the tension distribution for the values of the parameter Σ_e shown in Fig. 2.9. This shows that when Σ_e is small, the total tension around the circumference is almost constant at an arbitrary height $\tilde{z}$, but as Σ_e increases, the ratio of the tension generated at the top of the balloon to that generated near the bottom increases due to the effect of the film's own weight. The stress per unit length at the apex and base becomes infinite in the same manner as for the case of a pressurized balloon, which was described in the previous section.

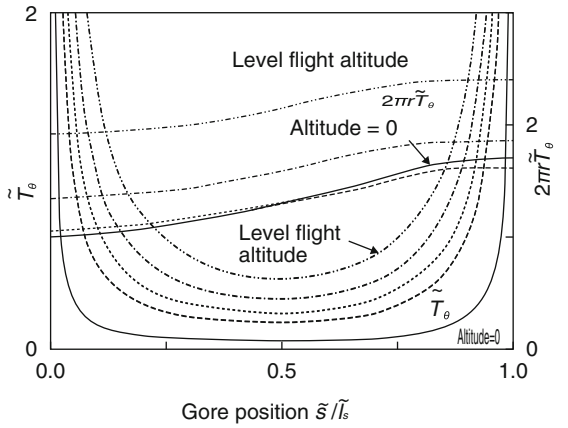

Fig. 2.10 Variation with altitude of the tension as a function of gore position. The *right axis* shows the total tensile force at a given gore position

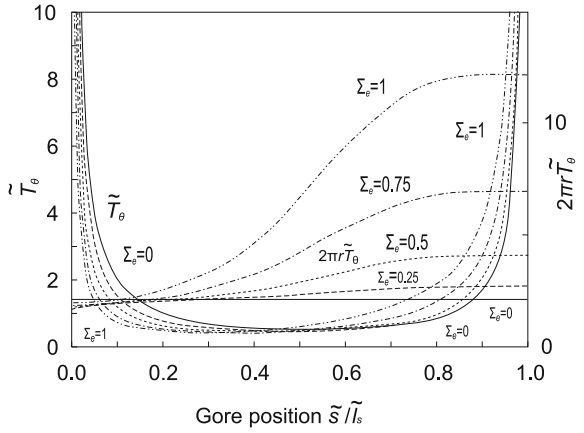

Fig. 2.11 Effect of Σ_e on the tension as a function of gore position. The *right axis* shows the total tensile force at a given gore position

The balloon model presented above is strictly mathematical, and, as such, it is not suitable for actual application in its current form. Because the circumferential length is zero at the apex and the base of the balloon, the film tension T_θ in the meridional direction becomes infinite, making it impossible to suspend a payload from the balloon.

In gore designs of early balloons, the cylinder end section or the taper-tangent end section was used for actual gore patterns (Fig. 2.12) to ensure that the circumferential length did not become zero. In other words, they were constructed so that folds or wrinkles were produced in the meridional direction at the top and

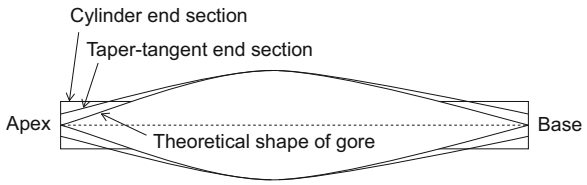

Fig. 2.12 Gore shapes that reinforce by increasing the amount of top and bottom film

bottom. As an extreme example, if both ends of a cylinder having a length equal to that of the balloon's meridional lines are tied, the length in the circumferential direction will be constant independent of the balloon height; hence, if the weight of the film is neglected, the circumferential tension will be constant, and will be independent of location. A load tape system was developed as a smarter design to solve this problem. The behaviors of balloons that have load tapes are discussed in the next section.

2.2.3 Expansion of Design Concepts for Balloons with Load Tape

2.2.3.1 Load Tape

With the exception of when light payloads of at most a few kilograms (such as radiosondes) are suspended, transmitting the concentrated load of a payload as a distributed load to the film is in a major problem in balloons that carry heavy devices ranging from a few hundred kilograms to in excess of 1 ton.

The load tape systems employed in typical scientific balloons made of polyethylene film involve the vertical insertion of reinforcing fibers along the sealing lines of adjacent gores. The fibers are strong and have a sufficiently low extensibility compared with that of the film. The payload is suspended from the point where all the load tapes concentrate at the base. This is a smart configuration that transmits and distributes the payload weight to the film (Fig. 1.4).

Such a system is highly compatible with the shapes of original natural-shape balloons in which only the meridional length is regarded as a constraining condition and where only meridional stress is present. It is well suited to manufacturing processes that make balloons by joining gore boundaries by heat-sealing. In addition, since the load tape bears all of the meridional tension, the advantage of this system is that the film stresses at both the apex and bottom of the balloon do not become infinite as in the description in Sect. 2.2.2.

2.2.3.2 Design of Natural-Shape Balloons with Load Tape (3D Gore Design Concept)

Returning to the starting point, we consider a method for extending the Upson's natural-shape balloon concept to balloons with load tapes. His basic concept involves producing only uniaxial film tension assuming nostretching of the film.

Here we try to design a balloon in which a gore forms a bulge with a small circumferential local radius between adjacent load tapes. At the bulge, we first assume that the meridional gore length is long enough that wrinkles are produced in the film in the circumferential direction, or, equivalently, there is no meridional tension. It is further assumed that the gore width is the length of the curved bulge in the circumferential direction. That is, by applying the same analogy as the original natural-shape balloon model of Sect. 2.2.2, the meridional tension on the film is $T_\theta = 0$, and tension T_φ is produced only in the circumferential direction.

Assuming such a configuration (Fig. 2.13b), the forces in the meridional direction are supported by only N strands of load tape, and only uniaxial tension is generated in the film, similar to the situation for original natural-shape balloons having no load tape. However, the direction of the tension is 90° to that for the case when there is no load tape (Fig. 2.13a), and it is in the circumferential direction. As a result, the circumferential film tension transfers to the load tapes and pulls them outward. The load tape curvature is defined by this pull up force and load tape tension.

If considered this way, since only uniaxial tension is present in the film, the statically determinate problem is applicable even to balloons that have load tape [9]. The circumferential tension in the film depends on the local radius of curvature R_φ at the location, and it is expressed simply as

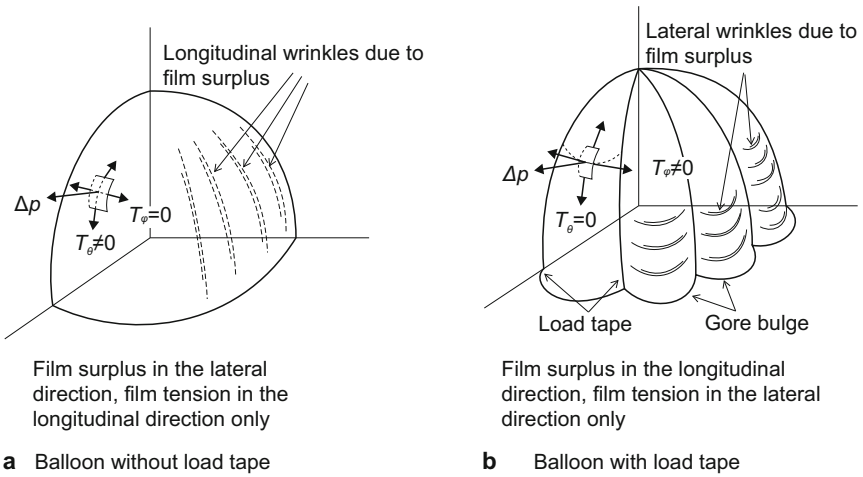

Fig. 2.13 Relationship between reinforcement and film tension resulting from load tape (partial diagrammatic view of upper quarter section): **a** Balloon without load tape (Film surplus in the lateral direction, film tension in the longitudinal direction only); **b** Balloon with load tape (Film surplus in the longitudinal direction, film tension in the lateral direction only)

$$T_\varphi = \Delta p R_\varphi, \tag{2.42}$$

where Δp is the difference between the internal and external pressures.

The radius of curvature R_φ may be selected independently of balloon size, and its minimum value is about half the length of the widest part of the spacing between adjacent load tapes. In other words, the radius of curvature R_φ governed by the number of load tapes N and the equatorial radius (i.e., the maximum circumferential radius) $r_{\max}$ of a balloon without load tape is given by the following equation,

$$\frac{R_\varphi}{r_{\max}} \geq \frac{\pi}{N}. \tag{2.43}$$

Thus, the radius of curvature R_φ may also be reduced to a few tenths of $r_{\max}$.

In addition, as will be discussed later, the load tape spacing is determined by the width dimension of the film material, which is packaged in a rolled condition at the time of manufacture. Therefore, to manufacture larger balloons, the number of load tape strands is just increased, while the spacing remains the same. According to (2.42), the film tension T_φ is independent of the balloon's size. This remarkable property is very different from that of conventional balloons, and is the key to being able to dramatically increase the pressure resistance of large balloons.

At the same time, the sum total of the tension T_ℓ applied to the load tape is also independent of balloon height. It is the product of the cross-sectional area at the balloon equator and the pressure differential Δp and is given by

$$NT_\ell = \pi r_{\max}^2 \Delta p. \tag{2.44}$$

From a different viewpoint, this tension is produced by the circumferential tension in the film pulling the load tape outward, and the tension generated in the film due to the pressure differential Δp is transferred as the load tape tension.

The 3D gore design concept is considered able to combine the functions of load tape and film to optimize the specific characteristics of both. A balloon structure based on this 3D gore concept is ideal for a natural-shape balloon having load tape, and it is an appropriate extension of the original natural-shape model to the case when load tape is inserted. As mentioned at the beginning of this section, to realize such a balloon it is necessary to construct a 3D shape so that each gore forms a bulge having a specific small local curvature [10].

2.2.3.3 Relationship to the Shape of Natural-Shape Balloons without Load Tape

The shapes of a balloon obtained by the 3D gore design concept and a balloon without load tape (which is considered in detail in Sect. 2.2.2) essentially share the following points.

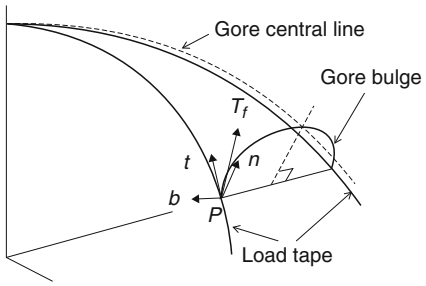

Fig. 2.14 3D gore cross-sectional shape and the direction of tension transferred to the reinforcing tape from the film

1. Inserting high-tensile-strength, low-extensibility load tapes along the meridian is consistent with the assumed conditions for a natural-shape balloon in which the meridional length is regarded as constant.
2. The meridional tension and the perpendicular force of the load tape, which determines its curvature, are both approximately proportional to those on the surface element of a balloon model without load tapes as described in Sect. 2.2.2. Then the load tape curvature is almost the same as the shape of the original natural-shape balloon.

Point (2) can be explained as follows. A segment of an infinitesimally wide strip is assumed to lie across the bulge between adjacent load tapes. The projected cross section of the strip is the product of the width and the load tape spacing. The force that pulls the load tape outward is equal to the product of this projected cross section of the small strip and the pressure exerted on the film. The meridional tension imparted to the load tape is equal to the product of the load tape spacing and the meridional film tension exerted on the surface element of a balloon model without load tapes, as shown in Fig. 2.7.

The slight difference between the two shapes is as follows. As shown in Fig. 2.14, a section orthogonal to the central line above the overhanging gore, and Cartesian coordinates **t**, **n**, and **b** are applied to the point P where this section intersects the load tape. **t** and **n** are normal to the tangent to the load tape. Because the gore section is not orthogonal to the load tape, the gore section tension T_f has not only a component in the **n** direction, but also a component in the **t** direction, and this deviates from the original natural shape without load tape.

This deviation is caused by the fact that the balloon is partitioned by a finite number (N) of strands of load tape. In large balloons where N is 100 or more, this difference can be neglected, but in small balloons this difference in shape has to be considered during design. The formulation is a little complicated, and we refer the reader to literature [10].

2.2.3.4 Implications of Reinforcement with Load Tape

Figure 2.15 shows a highly pressurized balloon reinforced by N strands of load tape by means of the 3D design concept. In unfurling the load tape at the apex and the bottom, it becomes arrayed like a cylindrical birdcage as shown in the figure. At

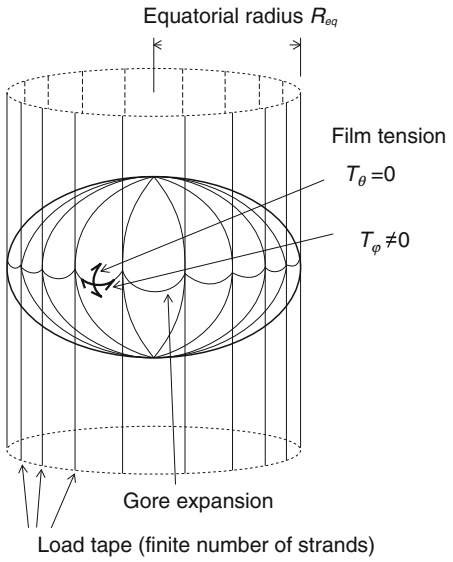

Fig. 2.15 Case of a finite number of load tape strands

this point, if the number of load tape strands is increased by a factor of n, the local radius of bulge curvature in the circumferential direction becomes $1/n$ due to film overhang, and hence, the tension decreases by $1/n$ in the same way. At this point, the quantity of load tape material is assumed to be the same, and one strand of tape is split vertically into n strands. In so doing, the tension and strength per strand of load tape both become $1/n$, and the load is uniform.

Furthermore, by repeating the same process, if n is increased to infinity, the film circumferential tension will tend to zero, and the load on the infinite strands of load tape will remain constant. If this balloon is unfurled, the infinite strands of load tape form an array in a cylindrical shape as shown in Fig. 2.16. That is, the infinite strands of load tape mutate into the film-like strong envelope material of the balloon, and the infinitely thin film functions as a gas barrier.

Consider the difference between two balloons: a balloon constructed by the cylinder as the limits of the above-mentioned 3D gore design concept and a balloon constructed by tying the top and bottom of a cylinder made only of film (Fig. 2.17). In the balloon made out of only film, since the amount of film in the circumferential direction is constant at every location, the film tension is also constant. The point of distinction is whether the material that makes up the envelope is film or high-tension fibers.

For a pressure vessel, the weight of the envelope generally decreases in inverse proportion to the specific strength of the envelope material, if the maximum pressure is kept the same. The specific strengths of the balloon film materials with good biaxial homogeneous characteristics are in the range of 3×10^3 to 6×10^3 m. By contrast, since a polymer fiber consists of long molecules aligned parallel to the fiber's axis, a high uniaxial specific strength can be obtained. Table 2.1 gives the specific strengths of representative high-strength polymer fibers, and they vary by about a factor of a

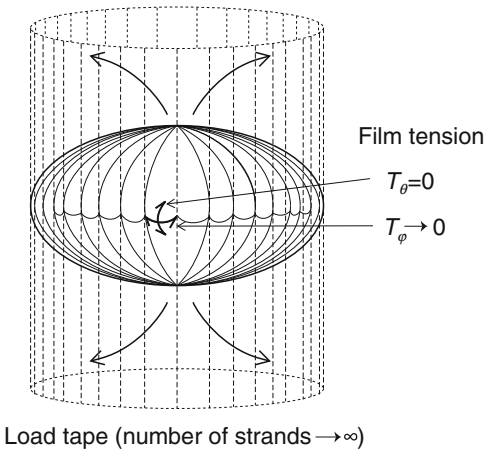

Fig. 2.16 Case when number of load tape strands tends to infinity

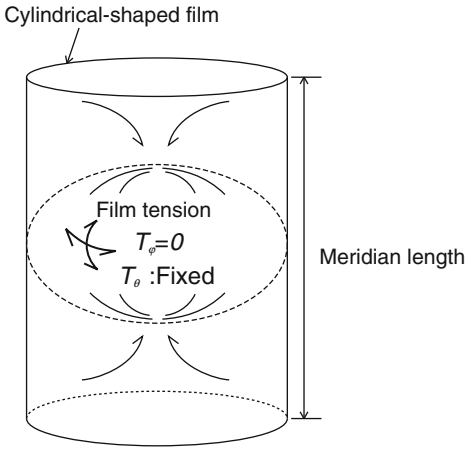

Fig. 2.17 Balloon made as a cylinder consisting just of film

Table 2.1 Specific strengths of representative high-strength fibers and balloon-use film

Material name	PBO	Aramid	High-strength polyethylene	Polyethylene film for balloon use
Specific strength ($\times 10^3$)	380	200	350	3–6

100 compared with polyethylene film for balloon use. An envelope constructed from these polymer fibers, under the constraint that the balloon weight remains constant, will have greater strength than a balloon made with polyethylene film according to the ratio of specific strengths.

The strength of a balloon reinforced with a finite number of strands of load tape is intermediate between the strengths of these two typical balloons (i.e., the film envelope and polymer fiber envelope). The 3D gore design concept offers the most effective reinforcement for balloons with load tapes.

More specifically, if we take R_{eq} to be the equatorial radius of curvature of the balloon constructed as a cylinder shown in Fig. 2.17, the film meridional tension T_θ when the pressure differential Δp is applied is given by

$$T_\theta = \frac{\Delta p R_{\mathrm{eq}}}{2}. \tag{2.45}$$

At the same time, for the balloon shown in Fig. 2.15, if the bulge is assumed to be semicircular, the maximum-value local radius on the equator $R_{\varphi,\max}$ is given by

$$R_{\varphi,\max} = R_{\mathrm{eq}} \sin\frac{\pi}{N}, \tag{2.46}$$

And the film circumferential tension T_φ is

$$T_\varphi = \Delta p R_{\varphi,\max}. \tag{2.47}$$

The ratio of the two tensions $K = T_\theta / T_\varphi \approx N/2\pi$ is the ideal reinforcement improvement rate from load tape. For example, if $N = 100$, then $K = 16$, and for $N = 200$, $K = 32$.

2.2.3.5 How to Construct a Balloon that has No Film Tension in the Meridional Direction

We consider how to make a gore having a 3D bulge from a planar film without elongating the film, so that, as in the description given in Sect. 2.2.3.2, the meridional tension $T_\theta = 0$ and the gore has a constant circumferential radius of curvature R_φ. As shown in Fig. 2.18, the width and length of the gore are made larger than that of conventional gore. At this point, the gore width of each part has a length that enables it to form a bulge of a specified radius of curvature R_φ between the adjacent load tapes. Here, if we make a planar gore, so that the centerline length of the gore is equal to that of the bulge, the length of the gore edges becomes longer than the load tape. Consequently, when manufacturing a balloon, the gore edges are joined to the relatively short load tape by gathering the edges. The excess film is then left in the meridional direction of the gore as circumferential wrinkles. At this juncture, by appropriately controlling the shortening proportion, a bulge that swells in a specified 3D shape can be formed from a planar-shaped gore. This process is similar to the 3D cutting procedures used for tailoring and dressmaking [11]. A model balloon with a volume of 3,000 m^3 was manufactured and tested to verify the 3D gore design concept.

The photograph in Frontispiece 5 shows an indoor full inflation test of the balloon.

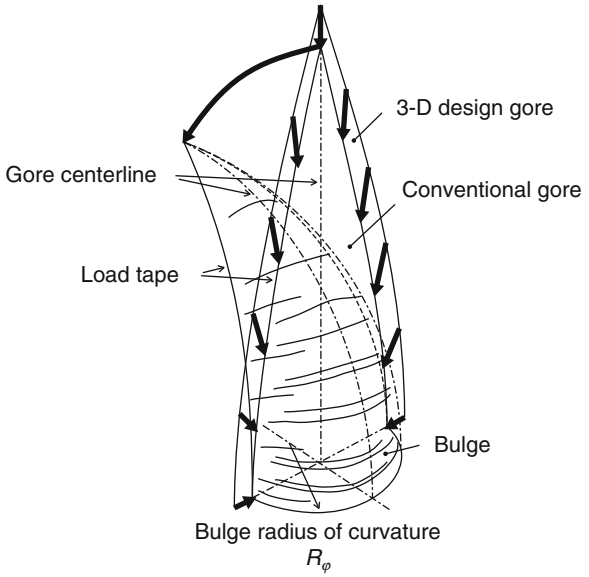

Fig. 2.18 Balloon-manufacturing method for the 3D gore design concept. A gore with a bulge is produced by attaching a gore that is larger than a conventional gore to the load tape by shortening (indicated by the *thick arrows*). This process is similar to the 3D cutting procedures used for tailoring and dressmaking

2.2.3.6 Problems with Conventional Balloons with Load Tape

In the design concept for a conventional balloon having load tape, N strands of load tape are attached at equal intervals to the surface of the natural-shape model having no load tape, as described in Sect. 2.2.2.2. The centerline length of the balloon gore is the meridian of the balloon, and the gore width is $1/N$ of the circumferential length. At the balloon manufacturing stage, the gores are joined to each other along their edges with load tapes.

In this manufacturing method, the length of the centerline of the gore is clearly shorter than the length of the junction line (i.e., the gore edge line). In the state where there is no pressure exerted and no extension in the film, the cross-sectional shape of the balloon becomes a polygon, as shown by line c in Fig. 2.19, and the load tapes are located at the vertices. In this state, the load tape subjected to the payload weight cannot be outwardly raised by film tension, and this configuration does not produce a balloon. Consequently, in an actual balloon, the gore must swell slightly outside the load tape due to its elasticity, as shown in Fig. 2.19b.

In this case, the gore must stretch not only in the circumferential direction, but also in the meridional direction. As biaxial elongation is required, the actual gore bulge due to the film's elasticity is further constrained. As a result, the circumferential radius of curvature near the centerline of the gore is not much smaller than the envelope radius, because the meridional stretching is required there and the tension

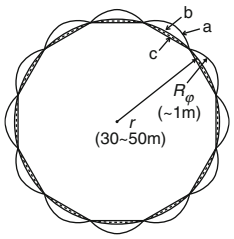

Fig. 2.19 Traverse cross-sectional diagram of a balloon envelope. Line c shows the normal gore cross-section. During full inflation, the shape bulges in the manner indicated by line b due to stretching of the film, and the radius of curvature near the gore centerline becomes about the same as the radius of circumferential curvature r of the balloon. Line a shows the swelled out position resulting from the 3D gore design concept, and the film in this case is not stretched

is generated in the meridional direction as well. This fact means that all the meridional forces are supported by both this film tension and the load tape tension. This phenomenon is not consistent with the design concept that the entire meridional force of the envelope should be supported by the load tape assembly having a high uniaxial tensile strength.

In addition, to utilize film extension for the realization of a balloon is different in principle from the Upson's natural-shape balloon model introduced in Sect. 2.2.2, and it is no longer a statically determinate problem. Accurate analysis of the biaxial film tension produced in this way is not straightforward, and finite element methods require numerical computation that extends to the case of flexible film materials having nonlinear properties. However, as an approximate estimate, the film tension at the burst point by pressurization is roughly the same as the tension on a sphere of the same volume. That is, with the 3D gore design concept, the film tension is proportional to the local radius of the bulge. In contrast with conventional balloons, the film tension is approximately proportional to the equatorial radius of the balloon. The observed burst pressures in flight-testing also support the same result.

With zero-pressure balloons (Sect. 2.3), the pressure differential applied is very small. In addition, the film deformations of a flat balloon gore are very small and are achievable due to the good elongation properties of polyethylene films used for balloons. As a result, while such a critical problem has not become evident in zero-pressure balloons, it is a major obstacle for realizing super-pressure balloons, in which the pressure differentials are particularly high.

A flight test of the 3,000-m^3-volume balloon shown in Frontispiece 5 was performed, and Fig. 2.20 shows photographs by an industrial television (ITV) camera installed in the payload looking up from underneath the balloon with a specified pressure differential after reaching the maximum altitude. In the enlarged photograph of Fig. 2.20b, the circular arc can be seen to bulge between the reinforcing tapes in accordance with the design idea of the 3D gore design concept [12]. Figure 2.21 shows a conventional shape for reference, but the differences are distinct in that the outer circumference is approximately circular, and there is no bulge between the load tape.

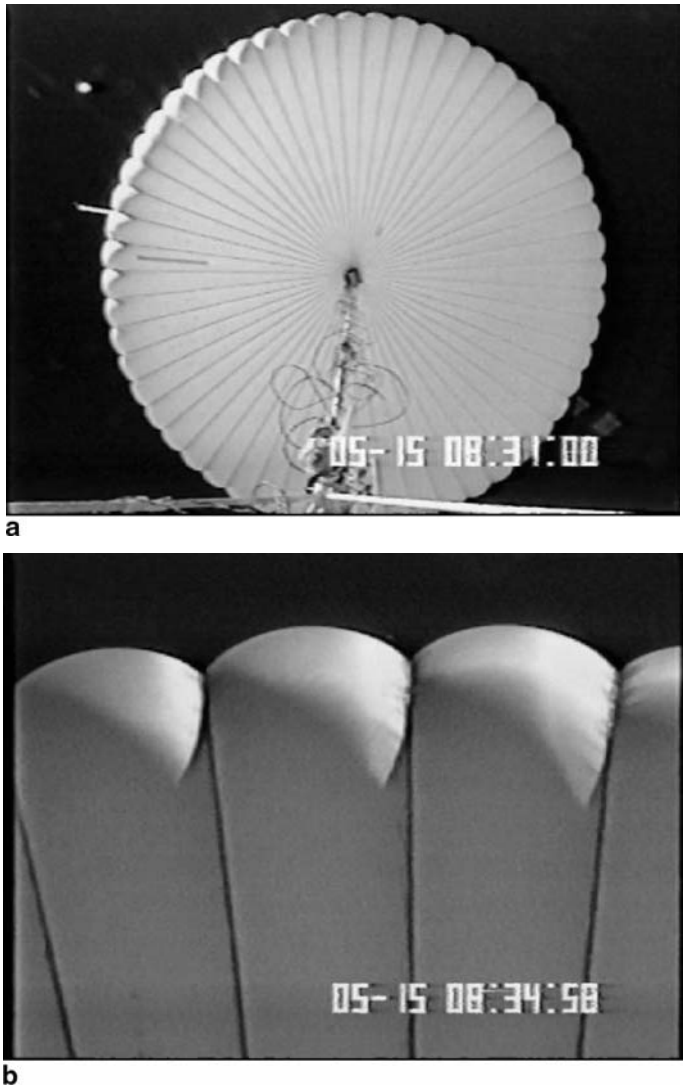

Fig. 2.20 Super-pressure balloon in flight. The bulges between the load tapes resulting from the 3D gore design concept are readily apparent: **a** Photograph of entire balloon; **b** Enlarged photograph

Table Talk 2: Another Natural-Shape Balloon Formulation

Dr. Jun Nishimura (former ISAS Director), who made profound contributions to scientific ballooning in Japan, worked independently on the formulation of a natural-shape balloon using variational methods. The variational method, based on certain constraining conditions, involves solving for extreme values of given functions (maximum or minimum value), and it is described in detail in physics textbooks.

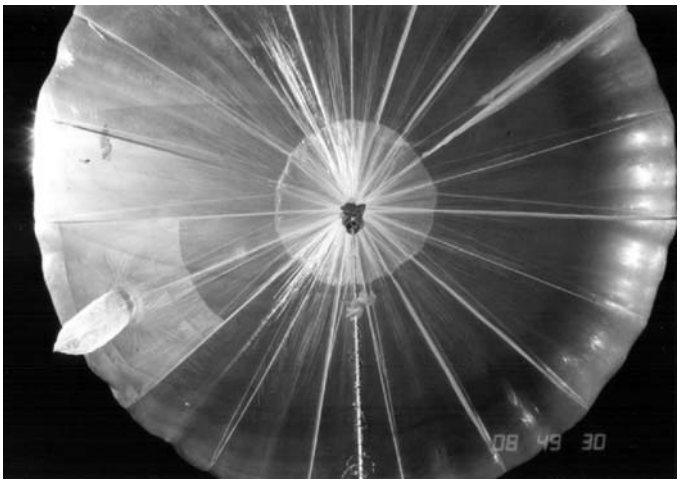

Fig. 2.21 Photograph looking up at a conventional balloon during ascent. Bulging ventilating duct just before exhaust is readily apparent

Dr. Nishimura assumed the two constraining conditions of constant meridional length and constant volume and determined the balloon shape as a function of the minimum potential energy of the buoyant force (the buoyant force point of action goes to the highest position). Although his approach differs from that of Upson, the results obtained were in agreement with the formula for a natural-shape balloon derived by Upson described in Sect. 2.2.2. Mathematically, it is the so-called "elegant solution" (i.e., the one having the simplest derivation).

Incidentally, why did the results of Upson, who determined the shape from the equilibrium of the forces acting on a surface element on the envelope, agree with the results of the variational method, which appears to be a completely different approach? There is a hint in the variational method constraint condition of keeping the meridional length constant. Here, the circumferential length has not been included as a constraint. That means the length is unrestricted. In other words, by considering the fact that there is excess film in the circumferential direction in the balloon in a partially inflated state, the condition that the meridional film tension is zero as conceived by Upson is incorporated as an initial assumption in the variational method.

Combining these two solutions, makes it easier to understand the fundamental properties of natural-shape balloons. More specifically, the balloon shape that generates tension in the film only in the meridional direction is also the shape in which the buoyant force produces the smallest potential energy.

2.3 Balloon Systems

In this section, we give an overview of the construction and functions of some representative balloon systems. Detailed in-flight characteristics for these systems are described in Sect. 2.4.

2.3.1 Zero-Pressure Balloons

Since zero-pressure balloons minimize the pressure on the balloon film, they opened the way to realizing large balloons constructed from thin, lightweight films. The half-century or so of modern scientific ballooning can be called the era of the giant zero-pressure balloon.

2.3.1.1 Construction

As mentioned in Sect. 2.2, zero-pressure balloons have a venting duct at the base of the balloon. After the balloon attains full inflation, if the lifting gas expands further it will overflow to the outside via the vent hole. Zero-pressure balloons are so termed because the internal–external pressure differential of the balloon is zero at the balloon base. Because the inside of the balloon is connected to the outside air through the venting duct, this type of balloon is also referred to as a balloon open to the air.

In reality, the venting hole is located a little higher up than the balloon base, and a duct is suspended from this hole to the base. In this configuration, the position of the venting hole is equivalent to the base. Since the ducts are constructed from the same flexible thin film as the balloon film, when the pressure in the base of the balloon exceeds that of the outside atmosphere, the duct is pushed open from the inside and forms a cylindrical shape, allowing the vent gas to flow smoothly through it. The photograph in Fig. 2.21 shows a venting duct in its inflated, venting state.

When the pressure differential is negative, the ducts are depressed down, thus preventing air flowing into the balloon. Consequently, the venting duct also functions as a check valve for one-way flow.

Ordinarily, the venting duct installed in the envelope hangs down naturally. However, if the balloon descends rapidly, there is a possibility that the bottom edge of the duct will float upward because of the air stream flowing on the side of the envelope. If this happens, the equivalent position of the vent hole will have been moved to a higher location; the lifting gas will be vented until the pressure differential at that position becomes zero. This reduces the buoyant force, and the balloon's descent may not terminate. Therefore, in cases when the flight plan includes a rapid descent, the venting duct is attached along the side of the envelope, as shown in Fig. 2.22.

2.3.1.2 Sustainability of Constant Altitude

After achieving its fully inflated condition, a balloon continues to ascend, maintaining the same volume while venting the lifting gas. Soon afterwards, the ascent stops at the altitude at which the buoyant force equals the weight of the total balloon system, and the balloon enters its level flight condition. In actual fact, the balloon continues to ascend even after the free lift becomes zero due its momentum. If the temperature difference between the lifting gas and atmosphere is neglected, there

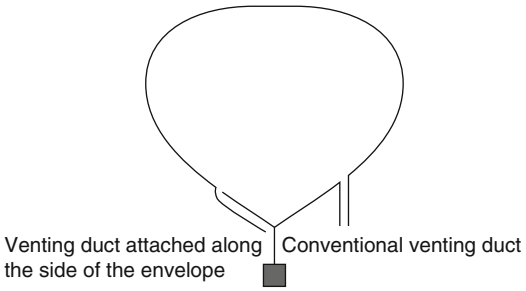

Fig. 2.22 Venting duct configurations

will be insufficient buoyant force due to excessive venting. After the balloon attains its maximum altitude, it will reverse direction and commence descending, and it will be unable to stop this descent.

As the details will be described in Sect. 2.4, however, essentially the temperature of the lifting gas during ascent is lower than that of the atmosphere because of the effect of adiabatic expansion. If ascent does stop, the gas temperature will increase to atmospheric temperature. This will compensate the reduction in the lifting force due to excessive venting, enabling the balloon to achieve a level flight.

On the one hand, under level flight conditions, if the buoyancy increases for some reason and the balloon starts to ascend again, lifting gas flowing from the venting duct will reduce the buoyancy, and the balloon will maintain a constant altitude. On the other hand, if the buoyancy decreases, the balloon will start to descend. If this occurs, its buoyancy will not recover since the increase in atmospheric pressure will reduce the volume of the balloon, and consequently the balloon will continue to descend.

In other words, if the temperature difference between the atmosphere and the lifting gas is ignored, zero-pressure balloons will have an automatic stabilization point when they ascend, but they will not have a stabilization point when they descend.

2.3.1.3 Altitude Compensation at Sunset

An important characteristic of zero-pressure balloons is the so-called sunset effect. As these balloons have a stable altitude only as they ascend, when the sun sets and they cease to absorb radiation from the sun, the temperature of the buoyant gas falls, buoyancy decreases, and the balloon can no longer maintain its altitude. If the internal balloon gas temperature decreases from T_g [K] by an amount ΔT_g [K] with the setting of the sun, the rate of buoyancy reduction due to contraction of the buoyant gas will be $\Delta T_g / T_g$.

The gas temperature of conventional polyethylene balloons flying over the earth's middle latitudes drops 15–25 K after the sun sets. Assuming the daytime gas temperature to be about 230 K, the reduction in buoyancy is about 7–10% of the total buoyant force. The weight of the payload must be reduced to compensate for this reduction in the buoyant force; this is done by dropping ballast with the aim of main-

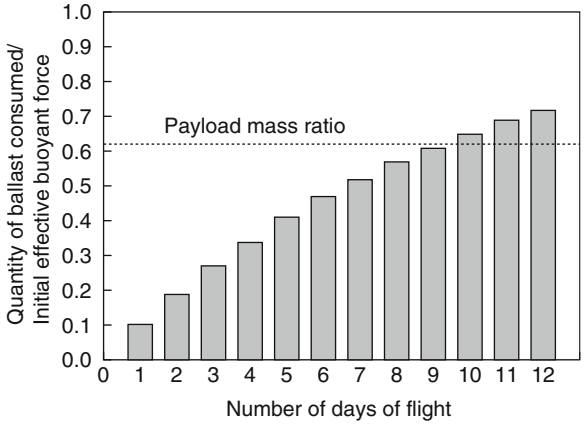

Fig. 2.23 Compensating for sunset and the number of flight days possible

taining the nighttime altitude. The gas temperature increases when the sun rises, and because the buoyancy recovers by an amount equivalent to the weight of the ballast dropped at sunset the previous day, the balloon starts to ascend again, and lifting gas is vented. At the next sunset, ballast is again dropped, and the cycle repeats. Since the total system mass m_t decreases with the dropping of ballast, the amount of ballast that needs to be dropped each day also decreases in proportion with the total system mass.

Let K_B represent the proportion of the quantity of ballast to drop each day to compensate for sunset relative to the total balloon system mass m_t. The total ballast consumption m_B for a flight of n days is then given by

$$m_B = m_t K_B \sum (1 - K_B)^{n-1}. \tag{2.48}$$

Figure 2.23 shows an example of how the total ballast consumption increases with the number of flight days, when K_B remains constant at 10% during an n-day flight. This example is for the case of a balloon with a volume of 100,000 m^3 flying in the stratosphere at an altitude of 31.2 km (atmospheric pressure: 10 hPa).

Assuming a standard atmosphere, the effective buoyancy force during level flight is approximately 12,850 N (refer to Appendix 1, "Standard Atmosphere Table"). The mass of the balloon for this volume is in the vicinity of 230 kg, and the inclusion of a parachute and other common equipment increases this figure to about 500 kg. Thus, the payload mass is about 810 kg, and it accounts for 62% of the initial effective buoyancy. Even if the entire payload were ballast, the number of flight days could not exceed 9 days according to Fig. 2.23.

2.3.1.4 Pressure Exerted on the Film

We denote the atmospheric pressure at the flight altitude as p_a and the density difference between the air and the lifting gas as $\Delta\rho$. If the temperature difference between

the lifting gas and air is ignored, the interior–exterior pressure differential Δp at a height z from the base of the balloon can be expressed as

$$\Delta p = \Delta\rho g z = \Delta\rho_0 g z \frac{p_\mathrm{a}}{p_{\mathrm{a}0}}, \tag{2.49}$$

where $\Delta\rho_0$ and $p_{\mathrm{a}0}$ are the differential gas density and the atmospheric pressure on the ground, respectively, and g is the acceleration due to gravity. Since $\Delta\rho_0$ is approximately $1.0\,\mathrm{kg/m^3}$, $p_{\mathrm{a}0}$ is $10^5\,\mathrm{Pa}$, and the balloon height is approximately 100 m. Thus, even for fully inflated large balloons, the interior–exterior pressure differential at the zenith is very small, being about only 1% of the atmospheric pressure p_a at the float altitude.

2.3.2 Super-Pressure Balloons

As this type of balloon does not require ballast to be jettisoned to maintain its flight altitude, long duration flights are unaffected by the sunset effect. Consequently, since the beginning of modern ballooning in the 1950s, many development projects have been carried out, and attempts at practical applications have been made. Although a high pressure resistance is required, the major aim of many trials was to develop strong lightweight balloon films to satisfy this requirement.

However, it is extremely difficult to practically produce a film that is able to withstand pressure differentials that are several factors of ten greater than those of zero-pressure balloons with only a few-fold increase in the weight of the film. The development of a super-pressure balloon has remained a subject of active research in balloon engineering for the past half-century or so. A fundamental solution to this problem is the "3D gore design concept," which is described in Sect. 2.2. Specifically, it is a shape design approach that attempts to find ways to reduce the tension produced in the film.

2.3.2.1 Construction

Unlike zero-pressure balloons described in Sect. 2.3.1, super-pressure balloons do not have a venting duct. That is, super-pressure balloons are closed to the outside atmosphere. The two exceptions to this are safety valves that operate automatically to release unexpected high pressures and/or exhaust valves that are opened and closed by remote operation from a ground base to control the buoyancy.

In principle, because the free-lift portion of the buoyant gas is not vented from the balloon, in order to stop the ascent of the balloon, the expansion of the free-lift portion of the gas must be constrained by the balloon film, and the pressure differential with the outside air will increase by this amount. Even when the diurnal change in the lifting gas temperature is considered, the pressure differential is about

20% of the atmospheric pressure at flight altitudes. Although the absolute value of this pressure differential may not appear to be very high in the low-pressure stratosphere, it is about 20 times higher than the pressure differential at the apex of a zero-pressure balloon, and for large-volume stratospheric balloons made from thin film, it is not a simple matter to withstand such pressures.

2.3.2.2 Sustainability of Constant Altitude

The free lift $\tilde{f} m_{\mathrm{t}} g$ is imparted to a balloon system having a total mass m_{t}, and the balloon expands while ascending. Here, $\tilde{f}$ represents the free lift ratio, which is defined as (free lift)/(total weight of balloon system) (see Sect. 2.4.2.2 for a more detailed explanation). As shown in Fig. 2.24, at an altitude of z_1 (balloon volume: V_{b1}, atmospheric pressure: p_{a1}, atmospheric density: ρ_{a1}) the pressure differential at the balloon base is zero (this is the zero-pressure balloon condition, State 1). The balloon's shape at this time corresponds to that shown by the shape c in Fig. 2.6, as described in Sect. 2.2. At this point, if the pressure gradient between the base and the apex of the balloon is ignored, the balloon's internal pressure p_{b1} will be the same as p_{a1}. After this, the pressure at the base increases as it gains altitude, and the shape of the balloon changes to the pumpkin shape depicted by the shape d to e in Fig. 2.6. Then, at an altitude of z_2 (balloon volume: V_{b2}, atmospheric pressure: p_{a2}, atmospheric density: ρ_{a2}, State 2) it attains its maximum altitude, and stops ascending.

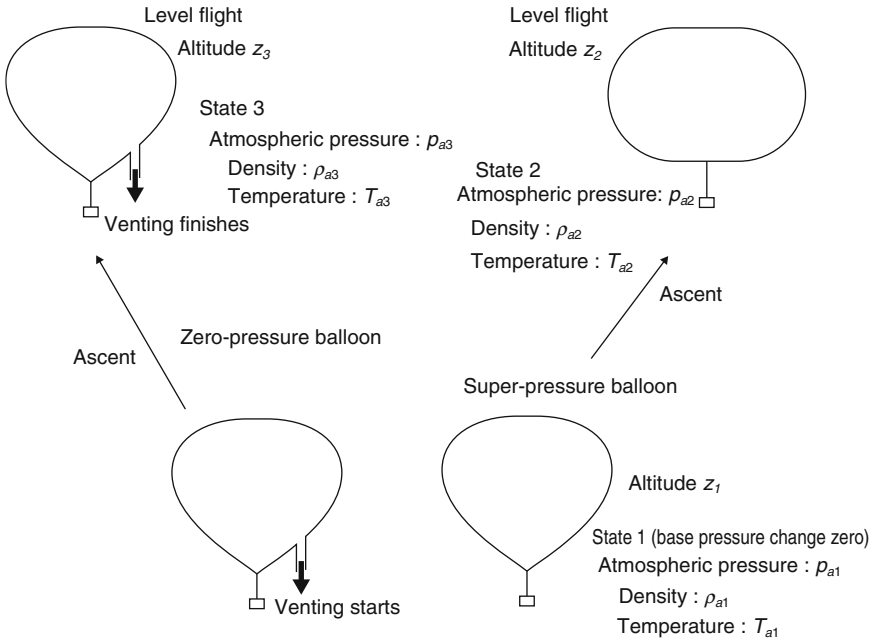

Fig. 2.24 Diagram showing balloon states

Subsequently, in the vicinity of this altitude, the volume of the balloon may be considered to be approximately constant. If the balloon climbs to an altitude higher than z_2, the air density decreases, and the buoyancy diminishes. Conversely, if its altitude decreases, its buoyancy will increase. In other words, in contrast to a zero-pressure balloon, a super-pressure balloon is stable in both the ascending and descending directions. Since it is not necessary to drop ballast to maintain altitude, long-duration flights become possible.

2.3.2.3 Pressure Exerted on the Film

The relationships between buoyancy, total balloon system mass, and balloon internal pressure in States 1 and 2 are given by

$$(1+\tilde{f})m_{\mathrm{t}}\frac{T_{\mathrm{g1}}}{T_{\mathrm{a1}}} = V_{\mathrm{b1}}\rho_{\mathrm{a1}}, \tag{2.50}$$

$$m_{\mathrm{t}} = V_{\mathrm{b2}}\rho_{\mathrm{a2}}, \tag{2.51}$$

$$\frac{p_{\mathrm{b1}}V_{\mathrm{b1}}}{T_{\mathrm{g1}}} = \frac{p_{\mathrm{b2}}V_{\mathrm{b2}}}{T_{\mathrm{g2}}}, \tag{2.52}$$

where T_{a1}, T_{a2}, T_{g1}, and T_{g2} are the atmospheric temperatures and lifting gas temperatures for States 1 and 2, respectively. In these two states, if the gas temperature and atmospheric temperature are equal, the balloon's internal pressure $p_{\mathrm{b2,0}}$ and its pressure difference with atmospheric pressure $\Delta p_{\mathrm{b2,0}}$ at level flight are both simply determined by the atmospheric pressure p_{a2} and the free lift ratio $\tilde{f}$ as expressed by the following equations.

$$p_{\mathrm{b2,0}} = p_{\mathrm{a2}}(1+\tilde{f}), \tag{2.53}$$

$$\Delta p_{\mathrm{b2,0}} = p_{\mathrm{a2}}\tilde{f}. \tag{2.54}$$

When there is a difference between the buoyant gas temperature and the atmospheric temperature, the internal pressure p_{b2} and the internal–external pressure difference Δp_{b2} are given by

$$p_{\mathrm{b2}} = p_{\mathrm{a2}}(1+\tilde{f})\frac{T_{\mathrm{g2}}}{T_{\mathrm{a1}}}, \tag{2.55}$$

$$\Delta p_{\mathrm{b2}} = p_{\mathrm{a2}}\frac{T_{\mathrm{g2}}\tilde{f}+(T_{\mathrm{g2}}-T_{\mathrm{a1}})}{T_{\mathrm{a1}}}, \tag{2.56}$$

Here, since the altitudes for States 1 and 2 are close, the respective atmospheric temperatures T_{a1} and T_{a2} can be treated as being equal. More specifically, the term $(T_{\mathrm{g2}}-T_{\mathrm{a1}})$ in the above equation is approximately equal to the temperature difference between the gas and the atmosphere for State 2, (i.e., $\Delta T_{\mathrm{g}} = T_{\mathrm{g2}}-T_{\mathrm{a2}}$). At night, the gas temperature T_{g2} falls more than the atmospheric temperature T_{a2}. When $\Delta p_{\mathrm{b2}} < 0$, the pressurization conditions as a super-pressure balloon are lost, and the balloon becomes a zero-pressure balloon and loses its altitude stability in the

downward direction. This boundary temperature $\Delta T_{\mathrm{g,lim}}$ is derived by substituting $\Delta p_{\mathrm{b2}} = 0$ into (2.56) as follows.

$$\Delta T_{\mathrm{g,lim}} = -T_{\mathrm{a2}} \frac{\tilde{f}}{1+\tilde{f}}. \tag{2.57}$$

Since the atmospheric temperature in the stratosphere is about 230 K, when $\tilde{f}$ is 8%, $\Delta T_{\mathrm{g,lim}}$ will be -17 K.

The gas temperature T_{g2} rises due to irradiation by the sun's rays. The phenomenon in which Δp_{b2} becomes greater than $\Delta p_{\mathrm{b2,0}}$ is called superheating, and it governs the balloon's design strength.

2.3.3 Special-Purpose Balloons

2.3.3.1 Dual-Balloon Systems

Super-pressure balloons described in Sect. 2.3.2 attempted to maintain a constant flight altitude by keeping a large balloon in a pressurized condition. Figure 2.25b and c depict dual-balloon systems, which are compound systems that combine a small super-pressure balloon and a large zero-pressure balloon, in which the volume of the zero-pressure balloon is K_v times greater than that of the super-pressure balloon. The small super-pressure balloon is used for controlling the altitude, while the large zero-pressure balloon is used for lifting the payload.

Systems that have been proposed include a tandem balloon, in which the balloons are situated above and below the payload (Fig. 2.25b), and a double-envelope

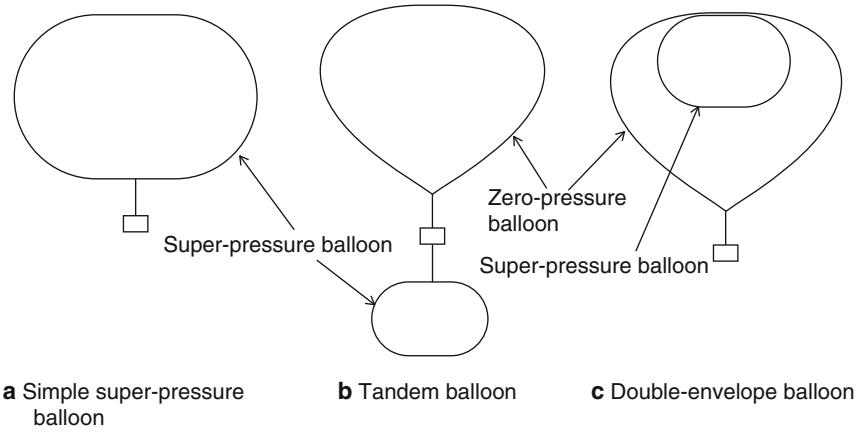

Fig. 2.25 Dual-balloon systems: **a** Simple super-pressure balloon; **b** Tandem balloon; **c** Double-envelope balloon

balloon (Fig. 2.25c). The former of these balloon designs has been tried by NASA, and it was named the Sky Anchor system [13].

In this balloon system, the reduction in the buoyancy of the zero-pressure balloon caused by the sunset effect is compensated by the increasing buoyancy of the super-pressure balloon as the flight altitude decreases. In other words, it differs from a simple super-pressure balloon in that it requires an altitude offset to maintain a stable flight altitude.

The pressure differential Δp of the super-pressure balloon increases to compensate for the change in the buoyancy of the large-volume, zero-pressure balloon. As shown in (2.58), the pressure differential Δp is a factor of K_v larger than that of a simple super-pressure balloon described by (2.54).

$$\Delta p = K_v p_a \tilde{f}. \tag{2.58}$$

In addition, the altitude offset Δz is given by

$$\Delta z = H_0 \ln \frac{p_{\min}}{p_{\max}}, \tag{2.59}$$

where $p_{\max}$ and $p_{\min}$ are the atmospheric pressures at the upper and lower altitude, respectively, and H_0 is the atmospheric scale height (Sect. 3.6.1). Figure 2.26 shows the relationship between the balloon volume ratio K_v and the altitude offset Δz for three different values of the buoyancy variation associated with the changes in gas temperature caused by the presence or absence of irradiation by sunlight.

The buoyant forces should be appropriately distributed between the two balloons, so that the zero-pressure balloon attains a state of zero pressure differential at the ceiling altitude. If we denote the buoyant forces of the zero-pressure balloon and the super-pressure balloon to be F_z and F_s, respectively, we obtain

$$F_z = m_t g - F_s, \tag{2.60}$$

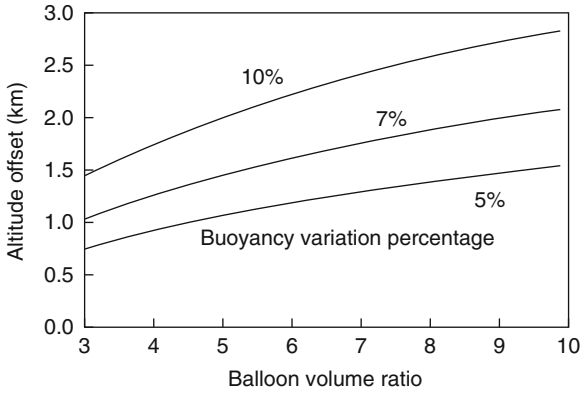

Fig. 2.26 Balloon volume ratio and diurnal variation in the flight altitude. The parameter in the figure is the ratio of diurnal buoyancy variation to total buoyancy

$$F_s = K_v m_t g \tilde{f}. \tag{2.61}$$

In this balloon system, the system weight of the super-pressure balloon can exceed its buoyant force, since the super-pressure balloon must be weighed down by the zero-pressure balloon to a certain degree to control the flight altitude in the manner described above. Thus, it is possible to avoid the strict constraint that the large simple super-pressure balloon must be made from a sufficiently lightweight film to enable it to reach the stratosphere while carrying a heavy payload. This permits a heavy film to be used for the envelope material, extending the range of films that can be used. Consequently, an improvement in the super-pressure balloon's manufacturability and reliability can be anticipated.

An additional advantage of this dual-balloon system is improved flight safety. Even if the super-pressure balloon bursts, the balloon system will not fall immediately because of the buoyancy of the zero-pressure balloon.

2.3.3.2 MIR Balloon

This is a balloon in which the optical properties of the balloon film have been designed in such a way that the buoyancy fluctuation associated with the presence or absence of solar radiation is minimized. Its development has been pursued since the 1970s by CNES, and it is referred to as a MIR balloon (Montgolfière Infrarouge, French for "infrared Montgolfier"). By enhancing the reflectivity of the upper half of the balloon, the increase in the buoyant gas temperature due to solar radiation is reduced, and by enhancing the infrared absorption of the lower half, the infrared energy radiated from the earth is absorbed reducing the drop in the gas temperature during the night. Although this balloon can transport only a light payload, and its diurnal altitude fluctuation can be as large as about 10 km, it has been able to perform long duration flights [14].

2.4 Motion of Balloons

In this section, we describe a flight model to illustrate the motion of balloons. To determine the motion of a balloon and its behavior during flight, it is necessary to model the temperature changes of the lifting gas inside the balloon, in addition to determining the forces acting on the balloon. To simplify the treatment, the balloon is treated as a point mass when considering the forces acting on the balloon. Pressure gradients within the balloon are ignored, and deformation or rotation of the balloon is not considered. However, when the effects of drag and pressure on the balloon are introduced to improve the accuracy of the model, it will be necessary to consider pressure gradients within the balloon and to take the balloon shape into account.

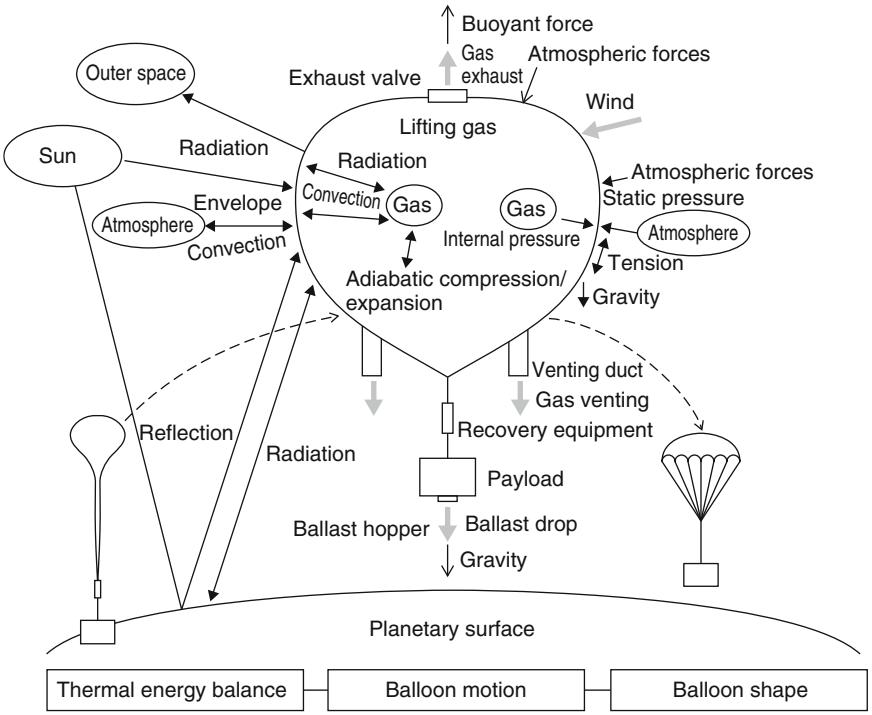

Fig. 2.27 Forces acting on a balloon and heat transfer into and out of a balloon

As shown in Fig. 2.27, the principal forces acting on the balloon are buoyancy, gravity, and the forces associated with the motion of the balloon and the relative motion of the atmosphere (subsequently, forces associated with the planet's atmosphere will be referred to as aerodynamic forces).

In addition, when taking the balloon shape into account, while there are internal and external pressure differences and tensions created within the envelope that vary with location on the balloon's surface, the impact of these fluctuations on the balloon's motion is small, and hence, they are not considered.

The following factors cause temperature changes in the balloon envelope and the lifting gas:

Adiabatic expansion and compression associated with

1. The aerodynamic force vector **F** acting on the balloon is expressed in terms of the relative wind velocity ambient atmospheric pressure changes due to the upward and downward motion of the balloon.
2. Convective heat transfer between the atmosphere and the envelope and between the lifting gas and the envelope.
3. Radiative heat transfer between the lifting gas and the sun, planet (earth), and space.
4. Radiative heat transfer between the envelope and the sun, planet (earth), and space.

The horizontal component of the balloon's speed and its speed relative to that of atmospheric winds are considered to be small.

First, in Sect. 2.4.1, we introduce a model that describes the balloon motion. Then, in Sect. 2.4.2, we give general expressions for the vertical motion of a balloon. We consider horizontal motion in Sect. 2.4.3, and the heat energy balance that critically affects the balloon motion in Sect. 2.4.4.

2.4.1 Balloon Flight Model

Consider the coordinate system depicted in Fig. 2.28, in which the z-axis is vertical and the x- and y-axes are orthogonal to the z-axis. Unit vectors parallel to the x-, y-, and z-axes are represented by **i**, **j**, and **k**, respectively. In addition, the balloon's position is denoted by $(x_\mathrm{b}, y_\mathrm{b}, z_\mathrm{b})$, its velocity vector is represented by $\mathbf{v}_b$ with components $(v_{\mathrm{b}x}, v_{\mathrm{b}y}, v_{\mathrm{b}z})$, and the wind velocity vector by $\mathbf{v}_w$ with components $(v_{\mathrm{w}x}, v_{\mathrm{w}y}, v_{\mathrm{w}z})$.

F has two components, namely, the drag force F_D that acts parallel to the relative wind vector, and the side force F_Y that acts perpendicular to the relative wind direction. More specifically,

$$F_\mathrm{D} = \frac{1}{2}\rho_\mathrm{a}\,|v_\mathrm{w} - v_\mathrm{b}|^2\, C_\mathrm{D} A_\mathrm{b}, \tag{2.62}$$

$$F_\mathrm{Y} = \frac{1}{2}\rho_\mathrm{a}\,|v_\mathrm{w} - v_\mathrm{b}|^2\, C_\mathrm{Y} A_\mathrm{b}, \tag{2.63}$$

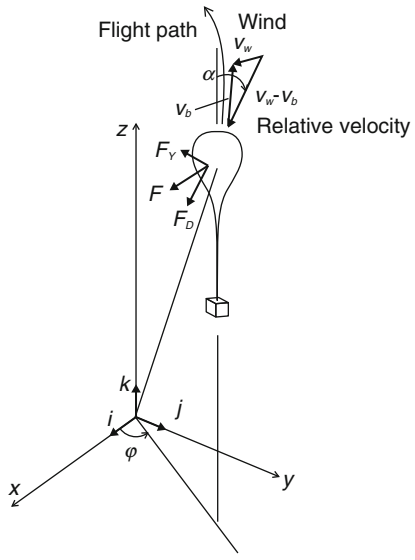

Fig. 2.28 Definition of coordinate system and aerodynamic forces acting on the balloon

where A_b is the standard area when calculating aerodynamic forces; this value is equal to the maximum cross-sectional area perpendicular to the balloon's axis and may be obtained by calculating the shape of the balloon. In addition, ρ_a is the atmospheric density.

The angle between the balloon's relative velocity vector $\mathbf{v}_b - \mathbf{v}_w$ and $\mathbf{k}$ is defined as the balloon's angle of attack α. C_D denotes the effective drag coefficient and C_Y is the effective side force coefficient, and these depend on the angle of attack α, the balloon shape, and the Reynolds number Re_b defined by the following equation

$$Re_b = \frac{\rho_a D_b |\mathbf{v}_w - \mathbf{v}_b|}{\mu_a}, \tag{2.64}$$

where D_b is the balloon's diameter, and μ_a is the coefficient of viscosity for air. The Reynolds number of the balloon Re_b is about 10^6–10^7 on the ground and about 10^4–10^6 at flying altitudes, depending on the magnitude of the buoyant force. Since a balloon is a membrane structure, it deforms slightly when it is acted on by aerodynamic forces, which modifies its drag coefficient and side force coefficient. In this case, however, deformation of the balloon by aerodynamic forces will be negligibly small. In the case of a 10-m-diameter balloon, for example, the internal–external pressure differential at the top of the balloon due to static pressure is about 100 Pa on the ground, whereas, the dynamic pressure on a balloon ascending at 5 m/s is an order of magnitude smaller, being about 15 Pa. In addition, the coefficients C_D and C_Y also include the air resistance originating from the uninflated lower part of the balloon. For large balloons that are usually used in the earth's stratosphere, C_D near the ground is of the order of 0.3.

If we take φ to be the angle between the vector $\mathbf{i}$ and the vector obtained by projecting vector $\mathbf{v}_w - \mathbf{v}_b$ onto the xy plane, and if we take F_x, F_y, and F_z to be the respective components in the x, y, and z directions of the aerodynamic force $\mathbf{F}$ acting on the balloon, we obtain

$$F_x = (F_D \sin\alpha + F_Y \cos\alpha)\cos\varphi, \tag{2.65}$$

$$F_y = (F_D \sin\alpha + F_Y \cos\alpha)\sin\varphi, \tag{2.66}$$

$$F_z = -F_D \cos\alpha + F_Y \sin\alpha. \tag{2.67}$$

At this point, for a balloon of mass m_b, a payload of mass m_p suspended from the bottom of the balloon, and ballast of mass m_c loaded therein, the balloon system mass (or the gross system mass) m_G is given by

$$m_G = m_b + m_p + m_c. \tag{2.68}$$

In addition, for lifting gas of mass m_g, the total balloon system mass m_t including the mass of the lifting gas is defined by

$$m_t = m_G + m_g. \tag{2.69}$$

The mass m_v is equal to the sum of m_t and the added mass determined by the direction of acceleration.

$$m_v = m_\mathrm{t} + C_\mathrm{m}\rho_\mathrm{a}V_\mathrm{b}. \tag{2.70}$$

Here the balloon's added mass coefficient C_m varies depending on the direction of the balloon's acceleration. For a sphere, it is 0.5, whereas for a zero-pressure balloon, vertical component of C_m varies from about 0.4 when the balloon is launched to 0.65 when the balloon has fully expanded. Conversely, the horizontal component of C_m decreases from 0.65 at the balloon launch to 0.4 when the balloon has expanded [15].

Based on the above, the equations of motion for the balloon are given as follows.

$$m_v \frac{\mathrm{d}^2 x_\mathrm{b}}{\mathrm{d}t^2} = F_x, \tag{2.71}$$

$$m_v \frac{\mathrm{d}^2 y_\mathrm{b}}{\mathrm{d}t^2} = F_y, \tag{2.72}$$

$$m_v \frac{\mathrm{d}^2 z_\mathrm{b}}{\mathrm{d}t^2} = (\rho_\mathrm{a}V_\mathrm{b} - m_\mathrm{t})g + F_z. \tag{2.73}$$

If we assume an ideal gas, the atmospheric density ρ_a is expressed by

$$\rho_\mathrm{a} = \frac{M_\mathrm{a}p_\mathrm{a}}{RT_\mathrm{a}}, \tag{2.74}$$

where p_a is the atmospheric pressure, T_a is the atmospheric temperature, M_a is the average molecular weight of air, and R is the gas constant. If we assume that the lifting gas is an ideal gas, the balloon volume V_b can be expressed as

$$V_\mathrm{b} = \frac{m_\mathrm{g}RT_\mathrm{g}}{M_\mathrm{g}p_\mathrm{g}}, \tag{2.75}$$

where M_g, T_g, and p_g are the lifting gas' molecular weight, temperature, and pressure, respectively. In a zero-pressure balloon, p_g and p_a can generally be considered to be equal. For a volumetric venting rate e_1 from the venting duct installed in the bottom part of the balloon and a lifting gas volumetric exhaust rate e_2 from the exhaust valve installed in the apex of the balloon, the mass balance for the lifting gas is

$$\frac{\mathrm{d}m_\mathrm{g}}{\mathrm{d}t} = -\rho_\mathrm{g}(e_1 + e_2), \tag{2.76}$$

or equivalently,

$$\frac{\mathrm{d}m_\mathrm{g}}{\mathrm{d}t} = -\frac{p_\mathrm{g}M_\mathrm{g}}{RT_\mathrm{g}}(e_1 + e_2), \tag{2.77}$$

where

$$e_1 = c_1 A_1 \sqrt{\frac{2\Delta p_1}{\rho_\mathrm{g}}}, \tag{2.78}$$

$$e_2 = c_2 A_2 \sqrt{\frac{2\Delta p_2}{\rho_g}}, \tag{2.79}$$

where A_1 is the total cross-sectional area of the venting duct and A_2 is the total opening area of the exhaust valve. c_1 and c_2 are the respective flow rate constants that vary with number and shape and are equal to the product of the flow contraction coefficient and the rate coefficient. In addition, Δp_1 and Δp_2 indicate the pressure differentials between the lifting gas and the surrounding atmosphere at the end of the venting duct and at the opening of the exhaust valve, respectively.

The balloon system mass is reduced by dropping of ballast. The mass drop rate for the ballast is e_3. More specifically,

$$\frac{\mathrm{d}m_c}{\mathrm{d}t} = -e_3. \tag{2.80}$$

To determine the lifting gas temperature T_g, it is necessary to consider the heat flow into and out of the balloon. If the heat that flows into the balloon envelope and the lifting gas are denoted by q_e and q_g, respectively, the envelope temperature T_e and the lifting gas temperature T_g can be expressed by the following two heat transfer equations:

$$m_e c_e \frac{\mathrm{d}T_e}{\mathrm{d}t} = q_e, \tag{2.81}$$

$$m_g c_{pg} \frac{\mathrm{d}T_g}{\mathrm{d}t} = q_g + V_b \frac{\mathrm{d}p_g}{\mathrm{d}t}, \tag{2.82}$$

where m_e is the mass of the envelope (which is different from the mass of the balloon m_b), c_e is the specific heat of the envelope, and c_{pg} is the specific heat of the lifting gas at constant pressure. By using (2.75) and the following equation

$$\mathrm{d}p_a = -\rho_a g \mathrm{d}z, \tag{2.83}$$

which expresses the relationship between the atmospheric pressure and density described in Sect. 2.3.1.3, (2.82) may be rewritten as [16]

$$m_g \frac{\mathrm{d}T_g}{\mathrm{d}t} = \frac{q_g}{c_{pg}} - \frac{g M_a m_g T_g}{c_{pg} T_a M_g} \frac{\mathrm{d}z_b}{\mathrm{d}t}. \tag{2.84}$$

The first term on the right-hand side is the heat influx to the lifting gas, and the second term is the effect of adiabatic expansion (or compression). Further details about the above-mentioned q_e and q_g are given in Sect. 2.4.4.

2.4.2 Vertical Motion of Balloons

At this point we describe a basic flight in which a balloon ascends and floats.

2.4.2.1 Stable Floating Condition

When a balloon is in a stable floating condition at a certain altitude, (2.73) is the equation for simple static balance.

$$(\rho_a V_b - m_t)g = 0. \tag{2.85}$$

Treating the atmosphere as an ideal gas, this equation may be rewritten as follows by using (2.74) and (2.75).

$$\frac{m_t}{m_g} = \frac{M_a p_a T_g}{M_g p_g T_a}. \tag{2.86}$$

If we define the ratio of the molecular weights of the gasses $\tilde{M}$ here as

$$\tilde{M} = \frac{M_a}{M_g}, \tag{2.87}$$

an equation describing the general floating condition of a balloon is obtained from (2.86) as follows

$$\frac{m_t}{m_g} = \tilde{p}_g^{-1}\tilde{T}_g\tilde{M}, \tag{2.88}$$

where $\tilde{p}_g$ and $\tilde{T}_g$ are the lifting gas pressure and temperature dimensionalized by the pressure and temperature of the surrounding atmosphere, respectively.

$$\tilde{p}_g = \frac{p_g}{p_a}, \tag{2.89}$$

$$\tilde{T}_g = \frac{T_g}{T_a}. \tag{2.90}$$

In super-pressure balloons, $\tilde{p}_g > 1$, whereas in zero-pressure balloons and in partially inflated balloons, ordinarily $\tilde{p}_g = 1$, but even in the floating condition, the gas temperature and the surrounding atmospheric temperature are generally different. The floating condition for this kind of zero-pressure balloon is expressed by

$$\frac{m_t}{m_g} = \tilde{T}_g\tilde{M}. \tag{2.91}$$

If the lifting gas pressure and temperature are equal to the pressure and temperature of the surrounding atmosphere respectively, this simplifies to

$$\frac{m_t}{m_g} = \tilde{M}. \tag{2.92}$$

2.4.2.2 Motion in the Vertical Direction

The equation for motion in the vertical direction (2.73) can be rewritten as follows

$$\left(m_t + C_m m_g \tilde{M}\frac{\tilde{T}_g}{\tilde{p}_g}\right)\frac{d^2 z_b}{dt^2} = \left(m_g\tilde{M}\frac{\tilde{T}_g}{\tilde{p}_g} - m_t\right)g + F_z, \tag{2.93}$$

and if $\tilde{p}_\mathrm{g} = 1$, this becomes

$$\left(m_\mathrm{t} + C_\mathrm{m} m_\mathrm{g} \tilde{M} \tilde{T}_\mathrm{g}\right) \frac{\mathrm{d}^2 z_\mathrm{b}}{\mathrm{d}t^2} = \left(m_\mathrm{g} \tilde{M} \tilde{T}_\mathrm{g} - m_\mathrm{t}\right) g + F_z. \tag{2.94}$$

Here the first term on the right-hand side expresses the net upward force of the buoyant force excluding gravity, and this is referred to as the free lift. This force changes during the flight depending on the relationship between the atmospheric temperature and the lifting gas temperature and on changes in the balloon's volume.

The ratio of the free lift divided by the acceleration due to gravity to the total balloon system mass including the lifting gas is denoted by $\tilde{f}$.

$$m_\mathrm{g} \tilde{M} \tilde{T}_\mathrm{g} - m_\mathrm{t} = \tilde{f} m_\mathrm{t}. \tag{2.95}$$

In particular, the free lift when leaving the ground is expressed by $\tilde{f}_0 m_\mathrm{t} g$. When the balloon is leaving the ground, it is generally acceptable to consider the atmospheric temperature and the lifting gas temperature to be equal so that

$$m_\mathrm{g} \tilde{M} - m_\mathrm{t} = \tilde{f}_0 m_\mathrm{t}. \tag{2.96}$$

2.4.2.3 Balloon's Rate of Ascent and Free Lift

When a balloon ascends at a constant speed in still air (free lift is positive), (2.94) becomes

$$(m_\mathrm{g} \tilde{M} \tilde{T}_\mathrm{g} - m_\mathrm{t}) g + F_z = 0. \tag{2.97}$$

If we make use of the expression

$$V_\mathrm{b} = m_\mathrm{g} \frac{\tilde{M} \tilde{T}_\mathrm{g}}{\rho_\mathrm{a}}, \tag{2.98}$$

the balloon's rate of ascent is given by the following expression

$${v_\mathrm{bz}}^2 = 2 \frac{m_\mathrm{g} \tilde{M} \tilde{T}_\mathrm{g} - m_\mathrm{t}}{\rho_\mathrm{a} C_\mathrm{D} A_\mathrm{b}} g. \tag{2.99}$$

If the shape of the balloon can be approximated by a sphere, (2.99) becomes

$${v_\mathrm{bz}}^2 = 4 \left(\frac{2}{9\pi}\right)^{\frac{1}{3}} \frac{g}{C_\mathrm{D}} \left(\frac{m_\mathrm{t}}{\rho_\mathrm{a}}\right)^{\frac{1}{3}} \frac{(1+\tilde{f})\tilde{T}_\mathrm{g} - 1}{(1+\tilde{f})^{\frac{2}{3}} \tilde{T}_\mathrm{g}^{\frac{2}{3}}}. \tag{2.100}$$

The velocity when the balloon leaves the ground $v_{\mathrm{bz},0}$ may be obtained by setting $\tilde{T}_\mathrm{g} = 1$

$${v_{\mathrm{bz},0}}^2 = 4 \left(\frac{2}{9\pi}\right)^{\frac{1}{3}} \frac{g}{C_\mathrm{D}} \left(\frac{m_\mathrm{t}}{\rho_\mathrm{a}}\right)^{\frac{1}{3}} \frac{\tilde{f}_0}{(1+\tilde{f}_0)^{\frac{2}{3}}}. \tag{2.101}$$

In stratospheric ballooning, the fraction of free lift is usually expressed by the ratio of free lift to the balloon's system mass m_G. Hence, we introduce f, which is defined by

$$\tilde{f} m_{\mathrm{t}} = f m_{\mathrm{G}}. \tag{2.102}$$

This f is termed the free lift rate. Unless indicated otherwise, the free lift rate usually refers to free lift rate when leaving the ground, f_0. Furthermore, there is the following relationship between f_0 and $\tilde{f}_0$.

$$f_0 = \frac{\tilde{f}_0 \tilde{M}}{\tilde{M} - \tilde{f}_0 - 1}. \tag{2.103}$$

The following relationship holds when lifting gas is not vented,

$$f = \frac{\tilde{f} \tilde{M} \tilde{T}_{\mathrm{g}}}{\tilde{M} \tilde{T}_{\mathrm{g}} - \tilde{f} - 1}. \tag{2.104}$$

By making use of the free lift rate, the following equation can be used to express the balloon's rate of ascent instead of (2.100).

$${v_{\mathrm{bz}}}^2 = 4 \left(\frac{2}{9\pi} \right)^{\frac{1}{3}} \frac{g}{C_{\mathrm{D}}} \left(\frac{m_G}{\rho_{\mathrm{a}}} \right)^{\frac{1}{3}} \frac{(1+f)\tilde{M}\tilde{T}_{\mathrm{g}} - (f+\tilde{M})}{(\tilde{M}-1)^{\frac{1}{3}} \left[(1+f)\tilde{M}\tilde{T}_{\mathrm{g}} \right]^{\frac{2}{3}}}. \tag{2.105}$$

The velocity when leaving the ground $v_{\mathrm{bz},0}$ is obtained by setting $\tilde{T}_{\mathrm{g}} = 1$ in (2.105).

For a stratospheric balloon, Fig. 2.29 shows the relationship between the free lift rate on the ground f_0 and m_G for different values of the balloon rate of ascent v_{bz}. The lifting gas is assumed to be helium and the drag coefficient of the balloon C_{D} is assumed to be 0.3. As m_G increases, f_0 decreases. During balloon ascent, the temperature of the lifting gas decreases due to adiabatic expansion. Since the second term on the right-hand side of (2.84) expresses this temperature change caused by adiabatic expansion (which becomes adiabatic compression during descent), the change in T_{g} attributable to only adiabatic expansion is expressed by

$$\frac{\mathrm{d}T_{\mathrm{g}}}{\mathrm{d}z} = -\frac{g\tilde{M}\tilde{T}_{\mathrm{g}}}{c_{\mathrm{pg}}}. \tag{2.106}$$

Using this equation, we consider the hypothetical case of ascent from a state in which there is no difference between the atmospheric temperature and the lifting gas temperature ($\tilde{T}_{\mathrm{g}} = 1$). By calculating the change in helium gas temperature with altitude, the temperature drop with altitude is found to be -13.7 K/km. In the same way, the temperature drop with altitude due to atmospheric adiabatic expansion for dry air is -9.8 K/km. The actual tropospheric temperature drop with altitude is low at -6.5 K/km, but this is due to the effects of water vapor (see Sect. 3.1.2 for a detailed explanation of changes in atmospheric temperature with altitude).

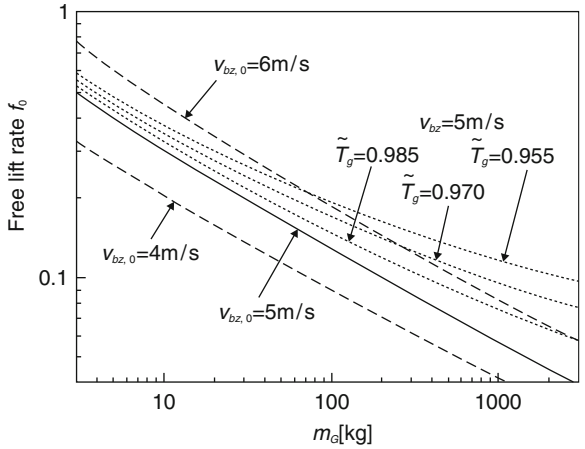

Fig. 2.29 Relationship between the balloon system mass and the free lift rate required to obtain a specified rate of ascent. The *solid line* and the *dashed lines* show the case when $\tilde{T}_g = 1$

In other words, based just on the effect of adiabatic expansion of the atmosphere and the lifting gas, the difference in the temperature drop with altitude is -7.2 to -3.9 K/km, and left this way, the temperature difference will increase with ascent. In reality, however, the lifting gas is warmed by convective flow with the atmosphere and by radiation. In addition, if the temperature of the lifting gas decreases, the buoyant force and rate of ascent will also decrease, counteracting the effects of adiabatic expansion. Because of these factors, the lifting gas temperature usually remains a few degrees below the atmospheric temperature when a balloon ascends.

By introducing this temperature drop, the free lift rate required for a certain balloon ascent speed (5 m/s) is indicated by the dotted line in Fig. 2.29. As for the lines shown in Fig. 2.29, at their respective ground conditions $\tilde{T}_g = 0.985$ corresponds to $T_g - T_a = -4.3^\circ$C; $\tilde{T}_g = 0.970$ corresponds to $T_g - T_a = -8.6^\circ$C, and $\tilde{T}_g = 0.955$ corresponds to $T_g - T_a = -13^\circ$C.

Ordinarily, the ratio of the heat loss due to adiabatic expansion to the heat influx by convective and radiative heat transfers increases as the cube root of the balloon volume. Therefore, if m_G increases, the increase in the free lift rate necessary to compensate the buoyancy loss caused by the temperature drop in order to obtain the required rate of ascent will become larger.

In fact, the free lift rate necessary to obtain a rate of ascent of 5 m/s in Fig. 2.29 is approximately equal to the curve shown at $\tilde{T}_g = 0.985$ when m_G is small, and it approaches the line $\tilde{T}_g = 0.970$ as m_G becomes larger. In other words, the lifting gas temperature for a normal balloon is about 5°C below the temperature of the surrounding atmosphere, and for large balloons exceeding 1 ton, it is more than 7°C lower.

As (2.100) shows, if the free lift rate does not change, the balloon rate of ascent is proportional to the $-1/6$ power of the atmospheric density, and it increases with altitude. In actual fact, however, the free lift rate due to adiabatic expansion given

above decreases in normal ascent. Consequently, there is no marked change in the rate of ascent for large balloons. This is because if the rate of ascent increases, the buoyancy decreases due to the increase in the temperature drop rate caused by adiabatic expansion resulting in a drop in the rate of ascent.

On the one hand, however, for the case when the reduction in the atmospheric temperature with height is very high (as when passing through the tropopause (see Sect. 3.1.2), for example), the rate of ascent decreases considerably due to the sudden increase in the temperature difference between the atmosphere and lifting gas. For details, refer to Sect. 2.4.4. On the other hand, in the case of small high-altitude balloons whose ratio of the volume at full expansion to that on the ground is around 1,000, after they clear the tropopause, the tendency for the rate of ascent to increase with altitude becomes stronger.

2.4.2.4 Balloon Floating Altitude

The line denoted a in Fig. 2.30 represents the variation in the atmospheric density with altitude. The horizontal axis is the logarithm of density. If we assume that for a balloon that is ascending the temperatures of the lifting gas and the atmosphere are the same ($\tilde{T}_\mathrm{g} = 1$), the balloon density ρ_b, which is defined by the following equation, is smaller than ρ_a by the amount of free lift, and the balloon ascends along the line labeled "b" in the figure.

$$\rho_\mathrm{b} = \frac{m_\mathrm{t}}{V_\mathrm{b}}. \tag{2.107}$$

The altitude at which the internal pressure of the balloon and the atmospheric pressure are equal is called the pressure altitude, and this point is regarded as State 1.

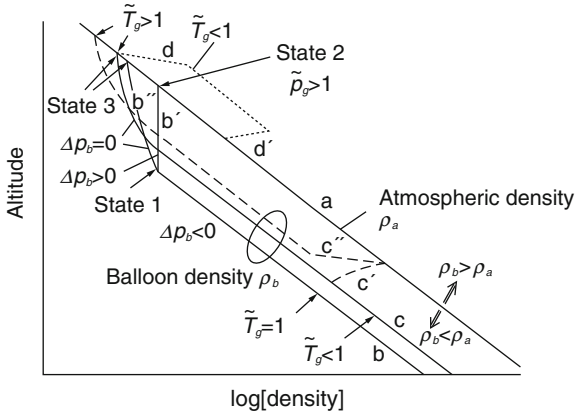

Fig. 2.30 Relationship between atmospheric density and balloon density when a balloon ascends and descends

On the one hand, for balloons such as super-pressure balloons that do not vent gas, the balloon continues to ascend still further from State 1, until the balloon density and the atmospheric density are equal. This point is called State 2. On the other hand, in the case of a zero-pressure balloon, ascent continues further from State 1 at constant V_b while venting the free-lift portion of lifting gas and maintains a constant altitude after $\rho_\mathrm{b} = \rho_\mathrm{a}$. The altitude at this point is called the density altitude, and it is regarded as State 3.

The density altitude when the lifting gas temperature and the atmospheric temperature are equal is called the isothermal density altitude, and it is determined by

$$\rho_{\mathrm{a}3} = \frac{m_G \tilde{M}}{V_{\mathrm{b}\max}(\tilde{M}-1)}, \tag{2.108}$$

where $V_{\mathrm{b}\max}$ is the balloon's maximum volume. However, usually, the lifting gas temperature is different from the atmospheric temperature, and the actual achievable altitude is given by

$$\rho_{\mathrm{a}3} = \frac{m_G \tilde{M}\tilde{T}_\mathrm{g}}{V_{\mathrm{b}\max}(\tilde{M}\tilde{T}_\mathrm{g}-1)}. \tag{2.109}$$

Next, during the ascent stage after leaving the ground until reaching State 1, at which the venting of lifting gas begins, the following equation holds

$$\rho_\mathrm{a} = \frac{m_\mathrm{t}}{V_\mathrm{b}}(1+\tilde{f}_0)\tilde{T}_\mathrm{g}. \tag{2.110}$$

This means that if $\rho_\mathrm{a} > \rho_\mathrm{b}$, i.e., $\tilde{T}_\mathrm{g} > 1/(1+\tilde{f}_0)$, the balloon ascends, and if $\rho_\mathrm{a} < \rho_\mathrm{b}$, i.e., $\tilde{T}_\mathrm{g} < 1/(1+\tilde{f}_0)$, the balloon starts to descend. Usually, because $\tilde{T}_\mathrm{g} < 1$ during ascent, the balloon ascends along line c, which lies closer to line a than to line b in Fig. 2.30.

The altitude of State 1 is

$$\rho_{\mathrm{a}1} = \frac{m_\mathrm{t}}{V_{\mathrm{b}\max}}(1+\tilde{f}_0)\tilde{T}_\mathrm{g} = \frac{m_G}{V_{\mathrm{b}\max}}\frac{1+f_0}{\tilde{M}-1}\tilde{M}\tilde{T}_\mathrm{g}. \tag{2.111}$$

For super-pressure balloons that do not vent gas, if the internal balloon gas pressure p_g is greater than the atmospheric pressure p_a, in other words, if

$$\frac{\tilde{M}(1+f_0)\tilde{T}_\mathrm{g}}{\tilde{M}+f_0} > 1, \tag{2.112}$$

then the achievable altitude will be nearly independent of the lifting gas temperature and will be given by

$$\rho_{\mathrm{a}2} = \frac{m_G}{V_{\mathrm{b}\max}}\frac{\tilde{M}+f_0}{\tilde{M}-1}. \tag{2.113}$$

Table 2.2 Differences in pressure altitude and density altitude

Density	$f_0 = 0.1$			$f_0 = 0.3$
	$\tilde{T}_g = 1$	$\tilde{T}_g = 0.95$	$\tilde{T}_g = 1.05$	$\tilde{T}_g = 0.95$
ρ_{a1}	1.276	1.213	1.340	1.433
ρ_{a2}	1.176	1.176	1.176	1.208
ρ_{a3}	1.160	1.170	1.152	1.170

When the lifting gas temperature drops (such as at night) in cases where the decrease in the internal pressure with the temperature drop is larger than the pressure proportion equivalent to the free-lift gas, the balloon is no longer a super-pressure balloon and has become a zero-pressure balloon.

As an example, Table 2.2 shows, for a stratospheric balloon, how the altitude (atmospheric density) changes for the cases when $f_0 = 0.1$ and $f_0 = 0.3$ in States 1–3. The atmospheric density (and hence the altitude) for each state may be determined by multiplying the values shown in the table by $m_G/V_{b\max}$. Specifically, if we assume that $m_G/V_{b\max} = 0.0073$, then for the case where $f_0 = 0.1$ and $\tilde{T}_g = 1$, the altitude difference between States 1 and 3 will be about 530 m, and the altitude difference between States 2 and 3 will be about 190 m. If the free lift rate becomes larger, for $f_0 = 0.3$ and $\tilde{T}_g = 0.95$, the altitude difference between States 1 and 2 will be about 1,300 m.

Usually, a balloon enters a level flight with a low temperature $\tilde{T}_g < 1$, and subsequently, because the gas warms, and the temperature rises during the day, the temperature becomes $\tilde{T}_g > 1$, and the balloon climbs slightly and once again enters a level flight; this is indicated by line c in Fig. 2.30. In Table 2.2, $\tilde{T}_g$ changes from 0.95 to 1.05.

2.4.2.5 Upward Motion Operation

Line c in Fig. 2.30 shows the case where ascent is stopped by forcibly exhausting gas through the exhaust valve during ascent. When ballast is subsequently dropped and the balloon climbs again (shown by line c in Fig. 2.30), the final float altitude increases. On the other hand, when the lifting gas temperature drops at night, the balloon starts to descend as indicated by line d in Fig. 2.30. The descent stops if ballast is jettisoned since the balloon density decreases as shown by line d in Fig. 2.30.

2.4.3 Horizontal Motion of Balloons

As shown in (2.71) and (2.72), balloon motion in the horizontal direction is governed by the aerodynamic forces produced by the difference between the velocity of the

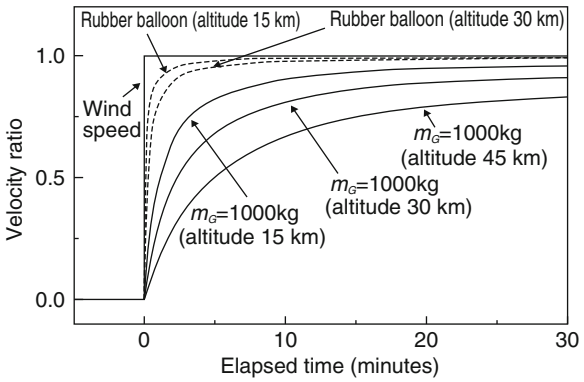

Fig. 2.31 Balloon motion when there is a step change in the speed of the surrounding wind

balloon in the horizontal plane and the wind velocity. If the wind velocity does not vary with time and location, this difference in velocity gradually disappears, and ultimately, the balloon moves at the same speed as the surrounding winds. However, since the wind varies with location, altitude, and time, as well as fluctuating abruptly, the horizontal motion of the balloon is not necessarily the same as the movement of the surrounding atmosphere. In particular, because a balloon at a high altitude has an extremely large volume, it is necessary to account for the slow response of the balloon to changes in the wind.

As a simple example, Fig. 2.31 shows how the speed of a balloon changes with time when the wind speed of the surrounding air changes suddenly by 2 m/s. For comparison, the motion of a radiosonde rubber balloon used in upper atmosphere observations (Sect. 3.6) is also shown.

The time required for a suddenly produced difference between the wind's velocity and the velocity of a small rubber balloon to diminish to 25% of its initial value is approximately 20 s at an altitude of 15 km, and even at an altitude of 30 km it is about 40 s. By contrast, the time required for a balloon having a balloon system mass of 1,000 kg is approximately 3 min at an altitude of 15 km and about 7 min at an altitude of 30 km, and this time extends to 15 min at an altitude of 45 km. While this is an extreme example, it is normal for balloons having diameters in the tens of meters or larger to require several minutes to acquire almost the same velocity vector as that of the surrounding wind. This means that a balloon ascending at 5 m/s will have ascended several kilometers by the time it changes direction.

2.4.4 Balloon Heat Balance

In this section, we describe the balloon heat balance that determines the temperature of the lifting gas. In other words, we determine q_e and q_g in (2.18) and (2.82). In the following description, "atmosphere" refers to the planetary atmosphere in which the balloon is flying, and "ground surface" means the ground surface of the planet.

As shown in Fig. 2.27, in addition to absorbing solar radiation, the envelope and lifting gas of a balloon flying in the atmosphere emit long-wavelength radiation into space and to the ground surface. In addition, the ground surface and atmosphere reflect part of the solar radiation energy, and along with infrared radiation from the ground surface, this radiation is partially absorbed by the balloon envelope and lifting gas. The reflection from the ground surface varies greatly depending on latitude, the condition of the ground surface, and whether or not there are clouds. In addition, there is heat transfer resulting from convective flow between the envelope and atmosphere and between the envelope and lifting gas. The radiative heat transfer between the envelope and lifting gas may be neglected since the temperature difference between them is small.

2.4.4.1 Envelope and Lifting Gas Heat Transfer

Here, we approximate the balloon as being spherical for simplicity, and denote its effective cross-sectional area as A_e, and its effective surface area as S_e. The heat flow into the balloon's envelope q_e and lifting gas q_g are given by the following equations, respectively

$$\begin{aligned} q_\mathrm{e} &= \tilde{\alpha}_\mathrm{e} I_0 (A_\mathrm{e} + F_\mathrm{bs} a_\mathrm{s} S_\mathrm{e}) + \tilde{\varepsilon}_\mathrm{e} \sigma S_\mathrm{e} (F_\mathrm{bs} T_\mathrm{s}^4 - T_\mathrm{e}^4) \\ &+ \tilde{\varepsilon} \sigma S_\mathrm{e} (T_\mathrm{g}^4 - T_\mathrm{e}^4) + h_\mathrm{ge} (T_\mathrm{g} - T_\mathrm{e}) + h_\mathrm{ae} (T_\mathrm{a} - T_\mathrm{e}) \end{aligned}, \tag{2.114}$$

$$\begin{aligned} q_\mathrm{g} &= \tilde{\alpha}_\mathrm{g} I_0 (1 + a_\mathrm{s}) S_\mathrm{e} + \tilde{\varepsilon}_\mathrm{g} \sigma S_\mathrm{e} (T_\mathrm{s}^4 - T_\mathrm{g}^4) \\ &+ \tilde{\varepsilon} \sigma S_\mathrm{e} (T_\mathrm{e}^4 - T_\mathrm{g}^4) + h_\mathrm{ge} (T_\mathrm{e} - T_\mathrm{g}) \end{aligned}, \tag{2.115}$$

where I_0 is the solar constant, and it is corrected depending on the altitude and the solar altitude, a_s is the reflectance of the ground surface (albedo), and it varies depending on the location of the balloon, the time, and whether or not there are clouds. $\tilde{\alpha}_\mathrm{e}$ is the effective solar absorptivity and $\tilde{\varepsilon}_\mathrm{e}$ is the effective infrared emissivity of the envelope; $\tilde{\varepsilon}$ is the effective emissivity between the envelope and lifting gas; and $\tilde{\alpha}_\mathrm{g}$ is the effective solar absorptivity and $\tilde{\varepsilon}_\mathrm{g}$ is the effective infrared emissivity for the lifting gas. T_s denotes the effective temperature of the ground surface viewed from the balloon, and it varies depending on the altitude, whether it is daytime or nighttime, and the cloud conditions. h_ge and h_ae are the convective heat transfer coefficients between the lifting gas and envelope and between the envelope and atmosphere, respectively. σ is the Stefan-Boltzmann constant. In addition, F_bs is the shape factor from the balloon to the planet, and it is 0.5 for a sphere.

If we consider the reflections from the balloon's interior, the effective emissivity and the effective absorptivity of the envelope and lifting gas can be determined using the following equations [16]

$$\tilde{\alpha}_\mathrm{e} = \alpha_\mathrm{e} \left(1 + \frac{\tau_\mathrm{e} (1 - \alpha_\mathrm{g})}{1 - r_e (1 - \alpha_g)} \right), \tag{2.116}$$

$$\tilde{\varepsilon}_{\mathrm{e}} = \varepsilon_{\mathrm{e}} \left(1 + \frac{\tau_{\mathrm{e}i}(1-\varepsilon_{\mathrm{g}})}{1 - r_{\mathrm{e}i}(1-\varepsilon_{\mathrm{g}})} \right), \tag{2.117}$$

$$\tilde{\varepsilon} = \frac{\varepsilon_{\mathrm{e}}\varepsilon_{\mathrm{g}}}{1 - r_{\mathrm{e}i}(1-\varepsilon_{\mathrm{g}})}, \tag{2.118}$$

$$\tilde{\alpha}_{\mathrm{g}} = \frac{\alpha_{\mathrm{g}}\tau_{\mathrm{e}}}{1 - r_{\mathrm{e}}(1-\alpha_{\mathrm{g}})}, \tag{2.119}$$

$$\tilde{\varepsilon}_{\mathrm{g}} = \frac{\varepsilon_{\mathrm{g}}\tau_{\mathrm{e}i}}{1 - r_{\mathrm{e}i}(1-\varepsilon_{\mathrm{g}})}, \tag{2.120}$$

where τ_{e} is the solar transmissivity of the envelope, $\tau_{\mathrm{e}i}$ is the infrared transmissivity of the envelope, r_{e} is the solar reflectivity of the envelope, $r_{\mathrm{e}i}$ is the infrared reflectivity of the envelope, α_{e} is the solar absorptivity of the envelope, $\alpha_{\mathrm{e}i}$ is the infrared absorptivity of the envelope, ε_{e} is the infrared emissivity of the envelope, α_{g} is the solar absorptivity of the lifting gas, and ε_{g} is the infrared emissivity of the lifting gas.

In reality, until the balloon is fully inflated, there is excess envelope (film) in the lower part of the balloon in the circumferential direction, and there are areas that overlap each other. As a result, the thickness differs depending on the location, and these equations become more complicated.

By using Nu_{a} and Nu_{g} to denote the Nusselt numbers for the atmosphere and the lifting gas, respectively, and the λ_a and λ_g to denote the thermal conductivities of the atmosphere and lifting gas, respectively, the convective heat transfer coefficients can be expressed by

$$h_{\mathrm{ge}} = \frac{Nu_{\mathrm{g}}\lambda_{\mathrm{g}}}{D_{\mathrm{b}}}, \tag{2.121}$$

$$h_{\mathrm{ae}} = \frac{Nu_{\mathrm{a}}\lambda_{\mathrm{a}}}{D_{\mathrm{b}}}, \tag{2.122}$$

where D_{b} is the balloon diameter.

The Nusselt number for the atmosphere for natural convection is given by

$$\begin{array}{l} Nu_{\mathrm{a}} = 2 + 0.589(Gr_{\mathrm{a}}Pr_{\mathrm{a}})^{1/4} / [1 + (0.469/Pr_{\mathrm{a}})^{9/16}]^{4/9} \\ (Pr_{\mathrm{a}} \geq 0.7,\ Gr_{\mathrm{a}}Pr_{\mathrm{a}} \leq 10^{11}) \end{array}, \tag{2.123}$$

and for forced convection, it is given by [17, 18]

$$Nu_{\mathrm{a}} = 2 + 0.03{Pr_{\mathrm{a}}}^{0.33}{Re_{\mathrm{b}}}^{0.54} + 0.35{Pr_{\mathrm{a}}}^{0.36}{Re_{\mathrm{b}}}^{0.58}. \tag{2.124}$$

If we consider the presence of natural convection within the balloon, the Nusselt number for the lifting gas is determined by [18]

$$Nu_{\mathrm{g}} = 0.54(Gr_{\mathrm{g}}Pr_{\mathrm{g}})^{1/4} \quad (Gr_{\mathrm{g}}Pr_{\mathrm{g}} < 2 \times 10^7), \tag{2.125}$$

$$Nu_{\mathrm{g}} = 0.135(Gr_{\mathrm{g}}Pr_{\mathrm{g}})^{1/3} \quad (Gr_{\mathrm{g}}Pr_{\mathrm{g}} > 2 \times 10^7), \tag{2.126}$$

where Gr_a and Gr_g are the Grashof numbers for the atmosphere and lifting gas, respectively, and Pr_a and Pr_g are the Prandtl numbers for the atmosphere and lifting gas, respectively.

With this, the equations describing balloon motion are complete. If (2.71) to (2.73), (2.114), and (2.115) are solved for specified initial conditions, it is possible to derive the balloon's behavior. In the next section, we look at the example of a stratospheric balloon over the earth and present a number of examples of calculations.

2.4.4.2 Ascending Motion

The two curves shown in Fig. 2.32 are a comparison of typical calculations for the cases of stratospheric balloons launched during the day and at night. The appropriate initial buoyancy is provided so that the average rate of ascent is about 5 m/s, and no ballast is dropped to correct the speed during flight.

The balloon ascends into the troposphere at roughly constant speed. When past the tropopause the atmospheric temperature drop ceases, and in due course it rises with altitude (refer to Sects. 3.1.2 and 3.1.3 for a detailed explanation of the structure of the stratosphere), but the temperature of the lifting gas continues to fall due to adiabatic expansion. Consequently, the temperature difference between the atmosphere and the lifting gas grows larger, and this results in a substantial drop in buoyancy. As the figure shows, the balloon's rate of ascent falls off in this vicinity. However, during the day, since there is sunlight, this temperature drop is gradually eliminated compared with that at nighttime as shown in Fig. 2.33a, and the temperature difference does not become much larger.

In addition, the aerodynamic forces in the vertical direction acting on a balloon are proportional to the balloon's cross-sectional area, and the buoyancy is proportional to the balloon's volume. Consequently, as the altitude increases, the upward

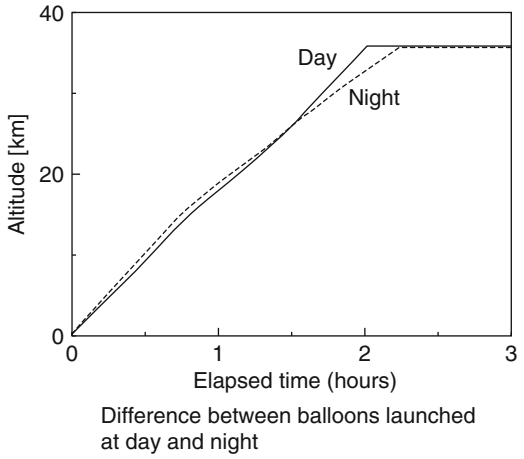

Fig. 2.32 Ascent of a zero-pressure balloon. Difference between balloons launched at day and night

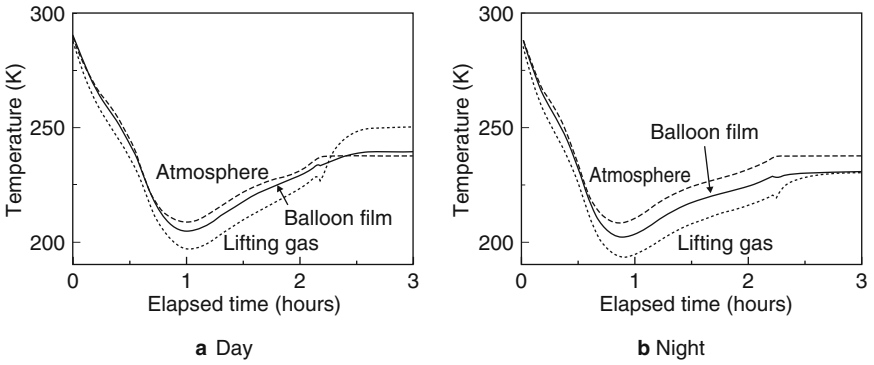

Fig. 2.33 Changes in atmospheric temperature, balloon film temperature, and lifting gas temperature. **a** and **b** correspond to day and night in Fig. 2.32, respectively:**a** Day; **b** Night

force increases in proportion to the third power of the balloon volume. This means that the rate of ascent increases in proportion to the 1/6-power of the balloon's volume. On the one hand, because of the combined effects of this and of sunlight, a balloon that slows down in the tropopause will start to gradually accelerate.

On the other hand, if a balloon ascends at night, since there is no supply of thermal energy from sunlight, as shown by the temperature changes in Fig. 2.33b, the temperature difference that begins in the tropopause does not diminish much. As a result, the balloon's rate of ascent beyond the tropopause does not increase very much. Hence, if there are cold clouds below, the slowing effect may be too large, and the balloon's rate of ascent may drop off greatly. Consequently, to avoid such excessive slowing, the free lift at night is often made larger than that during the day. In the calculation for the nighttime case shown in Figs. 2.32 and 2.33b, the free lift rate was increased by approximately 2% compared with that in the daytime.

2.4.4.3 Behavior Near the Float Altitude

Figure 2.34 is an enlargement of part of the altitude changes shown in Fig. 2.32. As shown in the figure, while the venting of the free-lift portion of the lifting gas starts a little below the float altitude, because the lifting gas temperature is lower than the atmospheric temperature, the balloon finishes venting and attains the float condition at an altitude lower than the isothermal density altitude. Subsequently, in accordance with the warming of the lifting gas, the balloon oscillates up and down a number of times and comes to rest at its final float altitude.

Venting of lifting gas is carried out a number of times in response to this oscillation. In the daytime case, because solar radiation induces a large increase in the temperature of the lifting gas, this up-and-down motion is usually small. However, these flight situations undergo various changes under different conditions. In the example shown in the figure, in the daytime case, the oscillation is small because the lifting gas temperature increases over the interval that gas is vented and the rate of

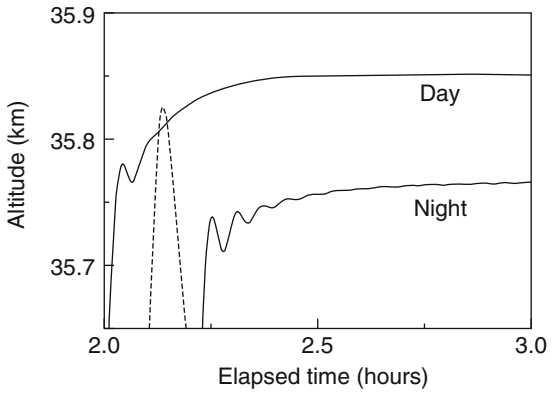

Fig. 2.34 Enlargement of Fig. 2.32 in the vicinity of where the at-float altitude is attained. The balloon reaches its level flight altitude by changing altitude up and down a few times as shown by the *solid line*. Venting of the lifting gas occurs 2–3 times in response. The *dashed line* shows the calculation results for the hypothetical case in which it is assumed that there is no temperature drop due to adiabatic expansion. Since the balloon ascends beyond its level flight altitude due to its inertial motion, there is excessive venting, and the balloon starts to descend after reaching its maximum altitude

ascent drops. However, the oscillations repeat in the nighttime example, since a long time is required for heat exchange with the atmosphere.

If there is no drop in gas temperature during ascent, and if we assume that $\tilde{T}_g = 1$ at all times, after the balloon reaches the float altitude, the balloon will ascend to a higher altitude due to inertial motion, and because lifting gas will be excessively vented, the balloon will commence to descend at a rate of approximately 1 m/s (as shown by the dashed line in Fig. 2.34).

2.4.4.4 Infrared Radiation Effects

Figure 2.35 shows the inflow and outflow of heat to the balloon film (envelope) and lifting gas term-by-term for the two calculations shown in Figs. 2.32 and 2.33.

It shows that, in contrast to the effect of adiabatic expansion, which remains approximately constant from immediately after launch until just before reaching float altitude, the quantity of absorbed radiation heat, while initially very small, gradually becomes larger as the altitude increases, and it exceeds the heat produced by adiabatic expansion. In particular, the absorption and radiation in the infrared region are shown to become even larger than the absorbed solar energy.

In the balloon's float condition, the energy absorbed from the sun, the infrared absorption from the ground, and the infrared radiation radiated to space are in equilibrium. In the float condition, provided the temperature does not change, the quantity of infrared radiation essentially does not change. However, if the condition under the balloon changes, the amount of infrared absorbed is expected to change greatly.

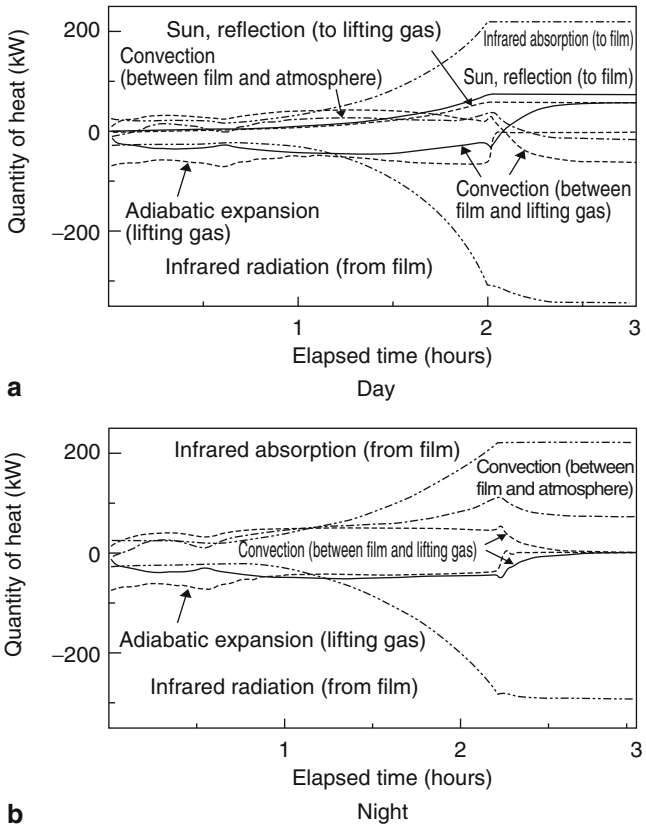

Fig. 2.35 Heat going into and out of balloon film and lifting gas. Figures **a** and **b** correspond to day and night in Fig. 2.32, respectively: **a** Day; **b** Night

A typical example of this is the difference between when there are no clouds under the balloon and when the area under the balloon is covered with cold clouds.

In the daytime, even if the area below the balloon is covered with clouds and the quantity of infrared radiation from below is reduced, since the reflection of solar radiation from the clouds compensates this decrease, the quantity of heat absorbed by the balloon film and lifting gas does not change greatly. Thus, the flight usually maintains a stable altitude. In contrast, since there is no solar radiation at night, if the area below is covered with cold clouds, the amount of infrared absorption drops off, and this is related directly to a drop in the balloon film's temperature.

Figure 2.36 shows calculation examples for this extreme case. In a period of 30 min, a balloon travels from a location where there are no clouds to a location where the area below the balloon is completely covered by clouds. The condition that the effective temperature T_s drops by 20°C continues for a while, as shown by the hatched region in the figure. In this kind of extreme case, the balloon loses substantial buoyancy and starts to descend. The final rate of descent reaches

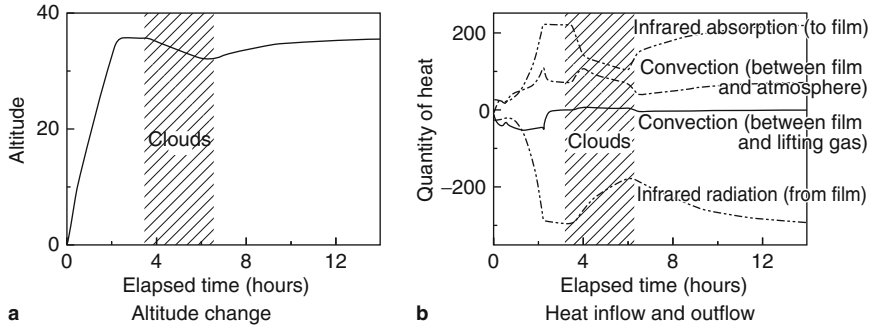

Fig. 2.36 Calculation results for a case where the area below the balloon is covered with cold clouds: **a** Altitude change; **b** Heat inflow and outflow

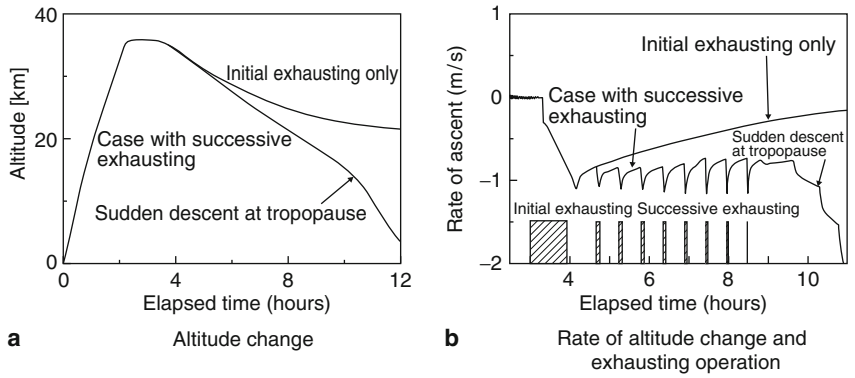

Fig. 2.37 Simulation results for descending from a float condition by opening the exhaust valve. Successive exhausting is required to descend at a fixed rate: **a** Altitude change; **b** Rate of altitude change and exhausting operation

0.3–0.4 m/s. However, if the clouds disappear and the infrared absorption is restored, the balloon stops descending, gradually turns around and starts to ascend again, but the speed of altitude recovery can be seen to be very slow, being about 0.1–0.3 m/s.

2.4.4.5 Descending Motion

To vary the altitude of a balloon that is in a level-flight condition, ballast is dropped to ascend, and lifting gas within the balloon is exhausted by opening the exhaust valve installed in the apex of the balloon to descend.

When descending by exhausting lifting gas from the exhaust valve, in contrast to the case for ascending, the temperature of the lifting gas increases due to adiabatic compression. Consequently, although it is assumed that a given rate of descent can be obtained by exhausting the required amount of gas to lose a certain amount of buoyancy, as the results of numerical simulations shown in Fig. 2.37 demonstrate,

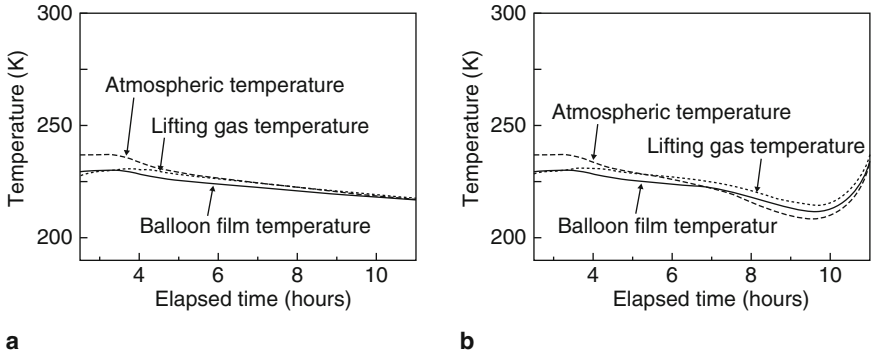

Fig. 2.38 Changes in atmospheric temperature, balloon film temperature, and lifting gas temperature. Figures **a** and **b** correspond, respectively, to the case when there is initial exhausting only and the case where successive exhausting is performed as shown in Fig. 2.37**a, b**

with just an initial exhausting, the gas temperature increases and the rate of descent declines, and ultimately, the descent may stop. The temperature change at this time is shown in Fig. 2.38a.

Consequently, successive exhausting is required to make the balloon descend at a constant rate. Since the valves normally used are not able to control the flow rate, exhausting is continued intermittently as shown in the bottom part of Fig. 2.37b in order to maintain an approximately constant rate of descent. The temperature of the lifting gas at this time rises above that of the surrounding atmosphere as shown in Fig. 2.38b.

The phenomena described above occur at altitudes higher than the tropopause. Since the temperature of the atmosphere rises when the flight altitude falls below the tropopause, it becomes difficult to stop the balloon's descent because the rate of descent rapidly increases even if the successive exhausting is terminated, as the example of successive exhausting shown in Fig. 2.37 demonstrates.

References

1. Archimedes, H.T.L. (ed): The Works of Archimedes, Dover Publications, New York, (2002)
2. Markhardt, T.: Recent Developments in the Use of Thin-Film Polyethylene Balloons for Meteorological Applications, AIAA Int. Balloon Technol. Conf., AIAA-91–3691-CP, 215–216 (1991)
3. Yamagami, et al.: Development of the Highest Altitude Balloon, Adv. Space Res., Vol. 33, No. 7, 1653–1659, (2004)
4. Prandtl, L., Tiejens, O.G., (Translated by Rosenhead, L.): Fundamentals of Hydro-and Aeromechanics, McGraw-Hill, New York, (1934)
5. Upson, R.H.: Stress in a Partially Inflated Free Balloon -with Note on Optimum Design and Performance for Stratosphere Exploration, J. Astronauti. Sci., Vol. 6, No. 2, 153–156 (1939)
6. Smalley, J.H.: Determination of the Shape of a Free Balloon, AFCRL-65–92, (1965)

7. Yajima, N.: Survey of Balloon Design Problems and Prospects for Large Super-Pressure Balloons in the Next Century, Adv. Space Res., Vol. 30, No. 5, 1183–1192 (2002)
8. Smalley, J.H.: Development of the e-Balloon, Proc 6th AFCRL Sci. Balloon Symp., 167–176 (1970)
9. Yajima, N.: A New Design and Fabrication Approach for Pressurized Balloon, Adv. Space Res., Vol. 26, No. 9, 1357–1360 (2000)
10. Yajima, N., et al.: Three Dimensional Gore Design Concept for High-Pressure Balloons, J. Aircr., Vol. 38, No. 4, 738–744 (2001)
11. Yajima, N., Izutsu, N.: Super-Pressure Balloon and Method of Manufacturing the Same, US Patent No. 6290172, (2001)
12. Izutsu, N., et al.: Flight Demonstration of a Superpressure Balloons by Three-Dimensional Gore Design, Adv. Space Res., Vol. 30, No. 5, 1221–1226 (2002)
13. Smith Jr., J.H.: Development of Sky Anchor Balloon System, Proc. 10th AFCRL Sci. Balloon Symp., 81–101 (1978)
14. Pommereau, J.P., et al.: First results of a Stratospheric Experiment Using a Montgolfiere Infra-Rouge (MIR), Adv. Space Res., Vol. 5, No. 1, 27–30 (1985)
15. Anderson, W.J., Shah, G.N., Park, J.: Added Mass of High-Altitude Balloons, J. Aircr., Vol. 32, 285–289 (1995)
16. Carlson, L.A., Horn, W.J.: New Thermal and Trajectory Model for High-Altitude Balloons, J. Aircr., Vol. 20, 500–507 (1983)
17. Incropera, F.R., de Witt, D.P.: Introduction to Heat Transfer, John Wiley & Sons, New Jersey, (1990)
18. Kutateladze, S.S., Borishanskii, V.M.: A Concise Encyclopedia of Heat Transfer, Pergamon Press, Oxford, (1966)

http://www.springer.com/978-0-387-09725-1

Scientific Ballooning
Technology and Applications of Exploration Balloons Floating in the Stratosphere and the Atmospheres of Other Planets
Yajima, N.; Izutsu, N.; Imamura, T.; Abe, T.
2009, XXI, 213 p., Hardcover
ISBN: 978-0-387-09725-1